

International Journal of Thermodynamics

Volume No. 28

Issue No. 3

September - December 2025



ENRICHED PUBLICATIONS PVT. LTD

**S-9, IInd FLOOR, MLU POCKET,
MANISH ABHINAV PLAZA-II, ABOVE FEDERAL BANK,
PLOT NO-5, SECTOR-5, DWARKA, NEW DELHI, INDIA-110075,
PHONE: - + (91)-(11)-47026006**

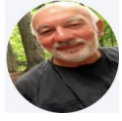
International Journal of Thermodynamics

Aims and Scope

The purpose and scope of the International Journal of Thermodynamics (IJoT) is

- to provide a forum for the publication of original theoretical and applied work in the field of thermodynamics as it relates to systems, states, processes, and both non-equilibrium and equilibrium phenomena at all temporal and spatial scales.
- to provide a multidisciplinary and international platform for the dissemination to academia and industry of both scientific and engineering contributions, which touch upon a broad class of disciplines that are foundationally linked to thermodynamics and the methods and analyses derived there from.
- to assess how both the first and particularly the second laws of thermodynamics touch upon these disciplines.
- to highlight innovative & pioneer research in the field of thermodynamics in the following subjects (but not limited to the following, novel research in new areas are strongly suggested):
 - Entropy in thermodynamics and information theory.
 - Thermodynamics in process intensification.
 - Biothermodynamics (topics such as self-organization far from equilibrium etc.)
 - Thermodynamics of nonadditive systems.
 - Nonequilibrium thermal complex systems.
 - Sustainable design and thermodynamics.
 - Engineering thermodynamics.
 - Energy.

Editor-in-Chief



Prof. Dr. Lütfullah KUDDUSİ
Istanbul Technical University

Thermodynamics and Statistical Physics, Experimental Methods in Fluid Flow, Heat and Mass Transfer, Computational Methods in Fluid Flow, Heat and Mass Transfer (Incl. Computational Fluid Dynamics), Electrochemical Energy Storage and Conversion, Microelectromechanical Systems (Mems), Heat Transfer in Automotive

Associate Editor-in-Chief

Assoc. Prof. Dr. Patrice ESTELLÉ
Université de Rennes

Associate Editor

Prof. Dr. Ali KOSAR
SABANCI ÜNİVERSİTESİ

Prof. Dr. Mustafa ÖZDEMİR
İSTANBUL TEKNİK ÜNİVERSİTESİ

Prof. Dr. Derya Burcu ÖZKAN
YILDIZ TECHNICAL UNIVERSITY

Assoc. Prof. Dr. Onur TAYLAN
ORTA DOĞU TEKNİK ÜNİVERSİTESİ,
MÜHENDİSLİK FAKÜLTESİ

Prof. Dr. Ahmet DURMAYAZ
İstanbul Teknik Üniversitesi

Prof. Dr. G. Reza VAKİLİ-NEZHAAD
Sultan Qaboos University

Prof. Dr. Ayşegül ABUŞOĞLU
İSTANBUL TEKNİK ÜNİVERSİTESİ

Prof. Dr. Ali Etem GÜREL
DÜZCE ÜNİVERSİTESİ, MESLEK

Prof. Dr. Bayram ŞAHİN
İSTANBUL TEKNİK ÜNİVERSİTESİ

Editorial Board

Prof. Dr. Yasar DEMİREL
It is not affiliated with an institution

Assoc. Prof. Dr. Abdussamet SUBASI
İSTANBUL TEKNİK ÜNİVERSİTESİ

Prof. Dr. Abel HERNANDEZ-GUERRERO
University of Guanajuato

Publishing Editor

Asst. Prof. Dr. Mustafa Yasin GÖKASLAN
VAN YÜZÜNCÜ YIL ÜNİVERSİTESİ

Res. Assist. Ali Murat BİNARK
İstanbul Teknik Üniversitesi

Res. Assist. Kasım ERDEM
İstanbul Teknik Üniversitesi

Language Editor

Assoc. Prof. Dr. Abdussamet SUBASI
İSTANBUL TEKNİK ÜNİVERSİTESİ

International Journal of Thermodynamics

(Volume No. 28, Issue No. 3, September - December 2025)

Contents

Sr. No	Article/ Authors	Pg No
01	A Detailed One Dimensional Finite-Volume Simulation Model of a Tubular SOFC and a Pre-Reformer* -Francesco Calise**,	1 - 19
02	Design of Evaporation Systems and Heaters Networks in Sugar Cane Factories Using a Thermoeconomic Optimization Procedure* -Adriano V. Ensinas**, Miguel A. Lozano;	20 -36
03	From Watt's Steam Engine to the Unified Quantum Theory of Mechanics and Thermodynamics -George N. Hatsopoulos	37 - 51
04	Thermodynamic Optimization of GSHPS Heat Exchangers* -Javad Marzbanrad**	52 - 62

A Detailed One Dimensional Finite-Volume Simulation Model of a Tubular SOFC and a Pre-Reformer*

Francesco Calise**, Massimo Dentice d'Accadia and Adolfo Palombo
DETEC-Università degli Studi di Napoli Federico II
P.le Tecchio 80- 80125 Naples. Italy.

Laura Vanoli
Dipartimento di Scienza degli Alimenti -Università degli Studi di Napoli Federico II
Via Università 100 - 80055 Portici (NA). Italy.

ABSTRACT

In this paper, a detailed model of a Solid Oxide Fuel Cell (SOFC) tube, equipped with a tube-and-shell pre-reformer unit, is presented. Both SOFC tube and pre-reformer are discretized along their axes. Detailed models of the kinetics of the shift and reforming reactions are introduced. Energy, mole and mass balances are performed for each slice of the components under investigation, allowing the calculation of temperature profiles. Friction factors and heat exchange coefficients are calculated by means of experimental correlations. Detailed models are also introduced in order to evaluate SOFC overvoltages. On the basis of this model, temperatures, pressures, chemical compositions and electrical parameters are evaluated for each slice of the two components under investigation. Finally, the influence of the most important design parameters on the performance of the system is investigated.

Keywords: Modelling, fuel cell, solid oxide fuel cell, SOFC, tubular SOFC, SOFC prereformer.

1. Introduction

Solid Oxide Fuel Cells (SOFC) can be considered one of the most efficient energy conversion devices for power production in stationary applications. In fact, the main peculiarities of such systems are: high electrical and thermal efficiencies, low pollutant emissions and reliability (Singhal et al., 2003). Presently, a number of types of SOFC are under investigation, namely: tubular, planar, tubular High Power Density (HPD) and microtubular (Singhal et al., 2003). Among them, the tubular configuration, developed by SiemensWestinghouse since the 1970s, can be considered as the most mature and reliable one (Larminie et al., 2004). Nevertheless, research must solve a number of issues before its commercialization, such as: cost targets, operating life, system optimization and integration with traditional devices (DOE, 2002).

In the last few years many researchers have been involved in the investigation of such systems by means of multi-scale approaches. In fact, many

* An initial version of this paper was published in July of 2006 in the proceedings of ECOS'06, Aghia Pelagia, Crete, Greece.

** Author to whom correspondence should be addressed.

papers are available in literature, dealing with the CFD or 0-D, transient or not, simulations of the SOFC stack and of power plants based on such technology (Singhal et al., 2003). Usually, CFD simulations are very time consuming both for model implementation and for calculation. On the other hand, 0-D simulations are much simpler and faster even if they cannot allow to determine parameter profiles (temperature, pressure, chemical composition, current density, etc.) within the component (Calise et al., 2004, Calise et al., 2006 a-c, Costamagna et al., 2001, Chan et al., 2002, Chan et al., 2003).

A number of 0-D models were previously implemented by the authors performing exergy analyses and optimization of hybrid SOFC power plants (Calise et al., 2004, Calise et al., 2006 ac). In these models, some simplifying assumptions were introduced in order to accomplish the evaluation of the electrochemical performance by using a 0-D approach (Calise et al., 2004, Calise et al., 2006 a-c). The following step of the research was the implementation of a finite-volume, axial-symmetric model of the SOFC stack, aimed at determining the profile of the most important design and operating parameters within the SOFC component and to assess the error due to the above mentioned simplifying assumptions (Campanari et al., 2004, Stiller et al., 2005). However, even in these papers a few simplifying assumptions were used, with reference to polarizations (for example, concentration is neglected in Stiller et al., 2005 and Ohmic overvoltage is calculated on the basis of a simplified series electrical arrangement in Campanari et al., 2004) and reforming reactions. In this paper, a novel approach for the axial-symmetric simulation of the SOFC tube is presented, taking into account the most detailed models available for polarizations, chemical kinetics and pressure drops. In the following, the simulation model is briefly presented, paying special attention to the results provided by the simulation.

2. System configuration

SOFC can convert the chemical energy of natural gas directly into electricity by means of the combined mechanisms of steam methane reforming and electrochemical reactions. In particular, the steam reforming process is achieved by using the steam produced by the electrochemical reaction (Singhal et al., 2003). In fact, the mixture required to support the steam methane reforming reaction can be easily

created by re-circulating SOFC anode outlet (Calise et al., 2006 c) 0.

In this paper, a SOFC stack with anode recirculation arrangement is investigated. This system consists of a number of sub-components such as: SOFC tubes, catalytic burner, mixers, ejectors, pre-reformer and heat exchangers (Calise et al., 2006 c). The operating principle of the internal reforming SOFC stack, equipped with an anode recirculation arrangement, was widely described in a number of previous papers (e.g. Calise et al., 2006 c).

SOFC tube is displayed in Figure 1, whereas its pre-reformer is shown in Figure 2. This latter component consists of a shell with a number of tubes filled with a proper catalyst for the steam methane reforming reactions. The heat required to support such reaction is supplied by the hot gases coming from the outlet of the stack combustor. Obviously, the stream coming out from the prereformer tubes is directly brought to the SOFC anode inlet.

In this work, the analysis is carried out only for the pre-reformer and SOFC tube that can be considered as the most complex components. Boundary conditions (air and fuel inlet temperature and chemical compositions) are derived from works previously developed by the authors (Calise et al., 2006 c). In future works, the 1-D model will be extended to the entire SOFC stack.

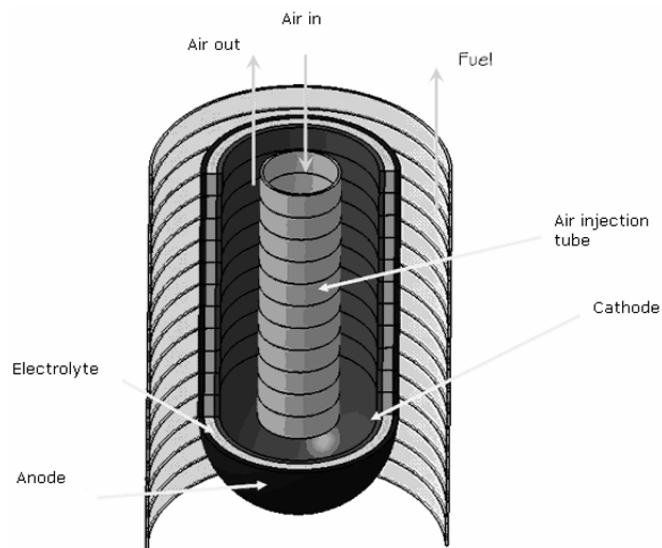


Figure 1. SOFC Tubular arrangement.

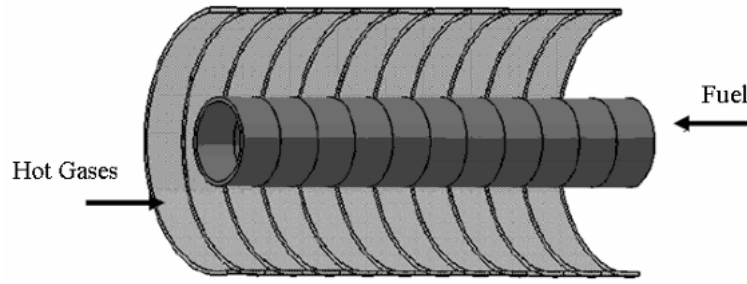


Figure 2. Pre-reformer configuration.

3. Electrochemical Model

SOFC voltage depends on a number of parameters, such as temperature, pressure, anode, cathode, electrolyte and interconnection thicknesses, porosity and tortuosity, materials, geometrical peculiarities, inlet chemical compositions, etc (Stiller et al., 2005). In order to consider all these factors, a detailed simulation model must be implemented. One of the aims of this paper is the development of a detailed simulation model to be used in order to verify the correctness of the simplifying assumptions, usually adopted in SOFC simulations. Previous works showed that some common simplifications, such as the use of the Tafel equation for the activation overvoltage or the use of the Fick's Law for the concentration polarization, should be avoided, since they may lead to significant errors, as shown in (Chan et al., 2001) and (Calise et al., 2004), respectively. In the present paper, detailed models for all the polarizations were implemented, as described in the following.

Obviously, cell voltage can be calculated evaluating Nernst open circuit reversible voltage (Larminie et al., 2004) and all the polarizations, according to the equation:

$$V = \frac{-\Delta \bar{g}_f^0}{2F} + \frac{RT}{2F} \ln \frac{p_{H_2} p_{O_2}^{1/2}}{p_{H_2O}} - \eta_{act,A} - \eta_{act,C} - \eta_{conc,A} - \eta_{conc,C} \quad (1)$$

Electron and ions transfer, respectively through electrodes and electrolyte, determine a loss due to their resistivities. Such property can be easily related to the operating temperature by means of exponential semi-empirical equations (Calise et al., 2006 a). Nevertheless, the calculation of the overall electric resistance is very complex since charges and ions flows occur both in radial and circumferential directions. Thus, the typical simplification of assuming a radial flow for electrons and ions (e.g.: Costamagna et al., 2001) was here avoided, by implementing more accurate relations such as those developed in (Nisanciooglu, 1989). The activation overvoltage, due to the energy barrier to be

overcome to activate the electrochemical reaction, is evaluated by means of the well-known Butler-Volmer (Calise et al., 2006 c). The exchange current densities (Singhal et al., 2003) are exponential function of temperature, are given in (Calise et al., 2006 c). Finally, the concentration overvoltage is due to the diffusion resistance of the porous media (anode and cathode). This phenomenon causes lower values of hydrogen and oxygen partial pressures, at the Three Phase Boundary, with respect to their corresponding values in the external flow (Larmine et al., 2004). Such overvoltage is related to the porosity of the electrodes and to the diffusion properties of the reacting mixtures (Chan et al., 2001). Usually, in the finite-volume simulation of SOFC the concentration overvoltage is neglected, since it is two orders of magnitude lower than other overvoltages, and modelling the concentration polarization is quite complex (Stiller et al., 2005). However, this assumption holds true only when the operating current density is lower than the corresponding limiting value 0. (Larmine et al., 2004) Hence, in some operating conditions (large values of the fuel utilization factor), the concentration overvoltage may become as large as the Ohmic and activation polarizations, as shown in Calise et all (2006 c). Thus, a complete polarization model should also include the concentration overvoltage in order to show all the phenomena that could occur in the SOFC tube (Chan et al., 2001). In this paper, the diffusion was considered as a combined mechanism of ordinary binary diffusion and Knudsen diffusion (Chan et al., 2001). The binary diffusion coefficient can be calculated on the basis of the Chapman-Enskog theory, also including the Lennard-Jones intercollision integral (Reid, 1977):

$$D_{AB} = 1,858 * 10^{-3} T^{3/2} \frac{\left[\frac{M_A + M_B}{M_A M_B} \right]^{1/2}}{p \sigma_{AB}^2 \Omega_D} \quad (2)$$

$$\Omega_D = \frac{A}{\left(\frac{kT}{\epsilon_{AB}} \right)^B} + \frac{C}{\exp\left(D \frac{kT}{\epsilon_{AB}} \right)} + \frac{E}{\exp\left(F \frac{kT}{\epsilon_{AB}} \right)} + \frac{G}{\exp\left(H \frac{kT}{\epsilon_{AB}} \right)} \quad (3)$$

Knudsen diffusion coefficient can be calculated on the basis of the theory of diffusion in a cylindrical pore, by means of the average pore radius, that can be related to the porosity, porous media area and bulk density (Reid, 1977; CEIC0010; Todd et al., 2002):

$$D_K = 97,0\bar{r} \sqrt{\frac{T}{M}} = 97,0 \frac{2\varepsilon}{S_A \rho_B} \sqrt{\frac{T}{M}} \quad (4)$$

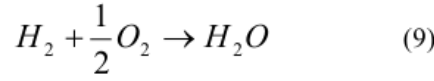
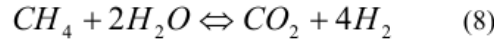
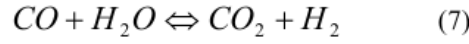
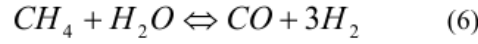
The actual overall diffusion coefficient can be calculated by considering material porosity and tortuosity and the combined mechanisms of ordinary and Knudsen diffusion, according with equation (5).

$$\frac{1}{D_{A,eff}} = \frac{\xi}{\varepsilon} \left(\frac{1}{D_{AB}} + \frac{1}{D_{AK}} \right) \quad (5)$$

Finally, the above calculated diffusion coefficient can be used in concentration equations in order to evaluate anode and cathode concentration over-potentials. In this paper, the theory developed by Chan et al. was used in order to evaluate both anode and cathode concentration overvoltages (Chan et al., 2001).

4. Reforming and Internal Reforming Model

The simulation of the reforming and internal reforming processes is usually carried out by implementing semi-empirical equations for the kinetic of the Steam Methane Reforming (SMR) reaction and by assuming equilibrium controlled the shift reaction (Calise et al., 2006 c). In order to avoid such simplifying assumption, in this paper a general theory, widely used in chemical process analysis, was implemented, by introducing relations that simultaneously include equilibrium and kinetic (Gallucci et al., 2004, Xu et al., 1989). This approach was used to simulate both prereforming and internal reforming processes. Furthermore, a special adjustment of the above mentioned model was performed, in order to simulate the internal reforming process. In fact, such approach was developed for the simulation of industrial reformers equipped with tubes filled with a proper catalyst. Conversely, in the SOFC the reforming reaction occurs at the thin anode layer that also consists of Ni (catalysts for the reforming reaction). Thus, the above mentioned approach (Gallucci et al., 2004, Xu et al., 1989) was properly calibrated and modified for the SOFC configuration, using an equivalent catalyst bulk density, in order to consider the catalyst mass that really participates in the reforming process. According to this approach, the SOFC overall process (internal reforming and electrochemical reaction) consists of reactions (6) to (9), whereas the pre-reforming process is carried out by reactions (6) to (8):



The rate of reaction (8) can be determined on the basis of the electrochemical model, as described in the following, whereas the rate of the three reforming reactions must be evaluated on the basis of the equations (10) to (14):

$$r_1 = \frac{\frac{k_1}{P_{H_2}^{2,5}} \left[P_{CH_4} P_{H_2O} - \frac{P_{H_2}^3 P_{CO}}{K_{eq_1}} \right]}{DEN^2} \quad (10)$$

$$r_2 = \frac{\frac{k_2}{P_{H_2}} \left[P_{CO} P_{H_2O} - \frac{P_{H_2} P_{CO_2}}{K_{eq_2}} \right]}{DEN^2} \quad (11)$$

$$r_3 = \frac{\frac{k_3}{P_{H_2}^{3,5}} \left[P_{CH_4} P_{H_2O}^2 - \frac{P_{H_2}^4 P_{CO_2}}{K_{eq_3}} \right]}{DEN^2} \quad (12)$$

$$DEN = 1 + K_{CO} P_{CO} + K_{H_2} P_{H_2} + K_{CH_4} P_{CH_4} + K_{H_2O} \frac{P_{H_2O}}{P_{H_2}} \quad (13)$$

$$k_i = A_i \exp\left(\frac{-E_i}{RT}\right) \quad (14)$$

The coefficients of equation (13) are given in literature (Gallucci et al., 2004, Xu et al., 1989). Equilibrium constants were calculated on the basis of the model previously developed by the authors (Calise et al., 2006 c). The rate of the electrochemical reaction was calculated on the basis of the electrochemical model, discussed in section 0. In fact, fixed the cell operating voltage, the polarization curve can be inverted in order to calculate current density. Such value can be used in a mole balance in order to evaluate the rate of the electrochemical reaction (Singhal et al., 2003):

$$r_4 = \frac{iA_{cell}}{2F} \quad (15)$$

Finally, from the above mentioned rates of reactions (equations from (9) to (14)), the outlet chemical composition were evaluated, by means of mole balances.

5. Pressure drops and heat exchange coefficients model

In this paper a pressure drop model was also included, based on the calculation of the friction factor depending on the Reynolds number. Correlations for friction factor are given in literature for all the streams included in the SOFC (Calise et al., 2006 c). The calculation of all the thermophysical properties (conductivity, viscosity, density, enthalpy, entropy, etc.) was based on the model previously developed by the authors (Calise et al., 2006 c). Similarly, correlations for the Nusselt number were implemented in order to evaluate all the heat exchange coefficients.

6. SOFC and pre-reformer discretizations and heat exchange models

In order to evaluate the profile of the most important parameters within the pre-reformer and the SOFC tube, such components were discretized along their axes, as shown in Figure 3 and Figure 4.

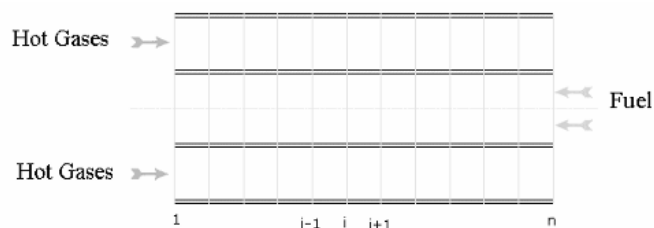


Figure 3. Pre-reformer discretization.

The typical tubular configuration of the SOFC, developed by Siemens is shown in Figure 1. The system consists of the cell, i.e. anode, cathode and electrolyte, and of an air injection tube required to supply air to the cathode compartment of the fuel cell. In this paper, a finite-volume axial-symmetric steady simulation of the SOFC tube was implemented. Consequently, border effects due to change of air flow direction in the bottom were neglected.

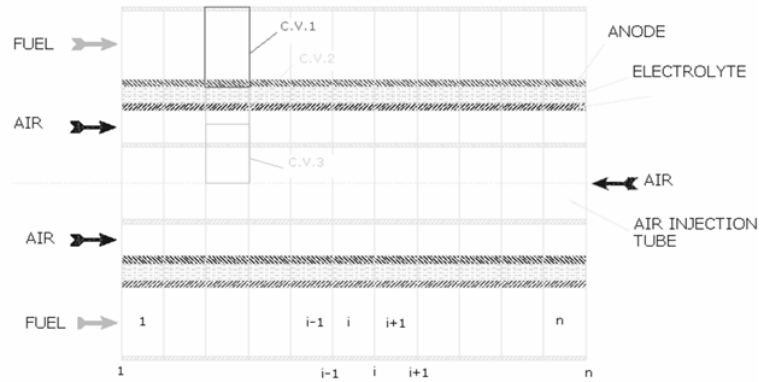


Figure 4. SOFC tube discretization.

The overall control volume was discretized by means of slices obtained with n plans orthogonal to the axis of the cylinders. Thus, the system was divided into n – slice (see Figure 4). The slice can be considered as the elementary volume of the discretization, and is reported on the x-axis of the following figures.

Similarly, the discretization of the prereformer was carried out.

Appropriate algorithms, written in MATLAB and TOMLAB, were developed both for SOFC tube and pre-reformer in order to determine the profiles of all the thermodynamic, chemical and electrical properties within those components. These algorithms were based on the above discussed chemical, electrochemical and pressure drops models coupled with the energy balance equations.

7. Results and discussion

7.1 Pre-reformer In theory, SOFC can also operate with a full internal reforming, i.e.: without any pre-reforming process. However, this circumstance should always be avoided, since the use of a pre-reformer provides several benefits. In fact this component is required to crack the higher hydrocarbons included in the fuel; in addition the pre-reforming promotes the internal reforming process and the electrochemical reaction. In fact, a cell not equipped with a pre-reformer would not produce any current at its bottom, since the corresponding active area would be used for the reforming process and not for the electrochemical reaction. It is also well-known that the reforming process occurring in the pre-reformer is strongly endothermic, resulting in a dramatic decrease of the fuel temperature. In fact the reforming process is much faster than the heat exchange between the reacting stream and the hot gases, determining the temperature profiles shown in Figure 5. Here, the active pre-reforming area is clearly detectable (from slice 80 to 100), also showing that the hot gases temperature variation is very low. In fact, the heat required to support the endothermic reforming process is mainly supplied by the

convective flow of the reforming stream.

TABLE I. INLET MOLAR FLOW RATES.

	SOFC		PR	
	Air	Fuel	Hot Gases	Fuel
H_2O (%)	0.0	26.8	8.8	44.4
CO (%)	0.0	11.1	0.0	4.8
H_2 (%)	0.0	33.3	0.0	7.1
O_2 (%)	21.0	0.0	11.3	0.0
N_2 (%)	79.0	0.6	75.5	0.8
CO_2 (%)	0.0	18.3	4.4	20.6
CH_4 (%)	0.0	9.8	0.0	22.2
tot (kmol/s)	3.75E-05	1.51E-06	1.02E-03	2.52E-04

All the results described in the following were calculated on the basis of the parameters fixed in TABLE I and TABLE II.

TABLE I shows the molar flow rate and chemical composition of inlet streams. Such data were calculated using the 0-D model previously developed by some of the authors (Calise et al., 2006 c, Calise et al., 2004). TABLE II shows the geometrical and operating parameters, which are similar to those of Siemens SOFC systems (Calise et al., 2004).

It is also well-known that high temperature gradients in the SOFC must be avoided. Thus, it is not possible to feed the stack with low temperature air and fuel. The air inlet temperature can be increased by means of an external pre-heater, supplied by the SOFC outlet stream. On the other hand, the fuel can be preheated by increasing the length of the prereformer, since this component also acts as a tube-in-tube counter-flow heat exchanger. However, the larger the length of the prereformer, the higher is the demethanization rate achieved in the same component.

Therefore, an increase in the pre-reformer length would result in a better heat exchange but also in a complete reforming process within such component. This circumstance must be avoided, since the internal reforming is crucial to provide additional cooling to the stack, avoiding unacceptable values of the stack temperature. Therefore, in the system under analysis the heat exchange was improved by adding a counterflow heat exchange between the hot gases and the fuel, in series with the pre-reforming

process, as shown in Figure 5. Here, it is also shown that a simple heat exchange process occurs in slices from 1 to 80, whereas combined heat exchange and steam reforming processes take place at slices from 81 to 100. This arrangement was achieved by filling with catalyst only a part of the pre-reformer tubes (slices from 81 to 100), so reducing their active length.

TABLE II. FIXED PARAMETERS.

Parameter	Unit	Value
Pre-reformer length	m	1.5
Pre-reformer active length	m	0.30
Pre-reformer fuel inlet temp.	°C	900
Pre-reformer hot gases inlet temp.	°C	1070
Pre-reformer tube diameter	cm	1.56
Pre-reformer wall thickness	cm	0.10
Pre-reformer catalyst bulk density	kg/m ³	1200
Cell Voltage	V	0.620
Anode thickness	cm	0.010
Cathode thickness	cm	0.220
Electrolyte thickness	cm	0.004
Interconnection thickness	cm	0.0085
Cell length	m	1.50
Interconnection versus cell area	/	0,097
Fuel inlet pressure	bar	3.00
Air inlet pressure	bar	3.00
SOFC Equivalent ρ_b	kg/m ³	0.60
Air inlet temperature	°C	900
Cell diameter	cm	1.56
Injection tube diameter	cm	1.20
Anode pore diameter	m	$0.5 \cdot 10^{-6}$
Cathode pore diameter	m	$0.5 \cdot 10^{-6}$
Anode porosity	%	50
Anode tortuosity	/	5.90
Cathode porosity	%	50
Cathode tortuosity	/	5.90
Anode conductivity	W/m K	2.00
Cathode conductivity	W/m K	2.00
Electrolyte conductivity	W/m K	2.00
Interconn.conductivity	W/m K	2.00

A simple energy balance returns that the higher the demethanization rate, the higher is the amount of heat required by the pre-reforming process. Reforming reaction kinetics are shown in Figure 7, where it is clearly displayed that the rate of the shift reaction, not equilibrium controlled as usually assumed, is mainly negative, whereas the reforming Steam Methane Reaction (eq. (5)) is much faster than the demethanization (eq. (8)). Figure 7 also shows that the steam methane reforming reactions are far from the chemical equilibrium. In fact, the chemical composition of the stream exiting the pre-reformer is very different from that of equilibrium. In addition, Figure 7 clearly shows that, at the pre-reformer outlet, steam methane reforming reactions are still in progress. Pressure profile plots are omitted since pressure drops are negligible. It is important to emphasize that the results achieved in Figure 7 could not be achieved by 0-D models.

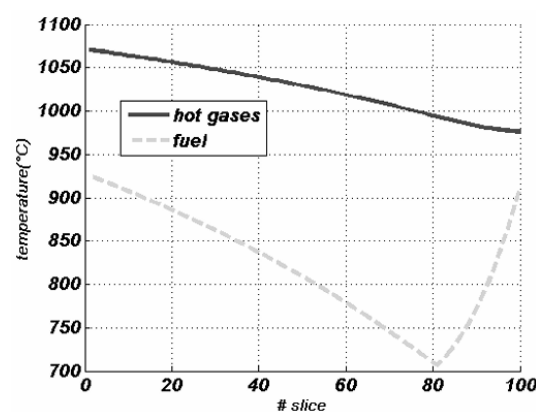


Figure 5. Pre-reformer temperatures.

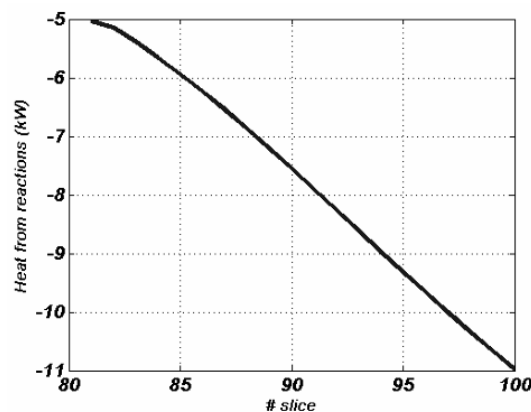


Figure 6. Pre-reformer heat from reactions.

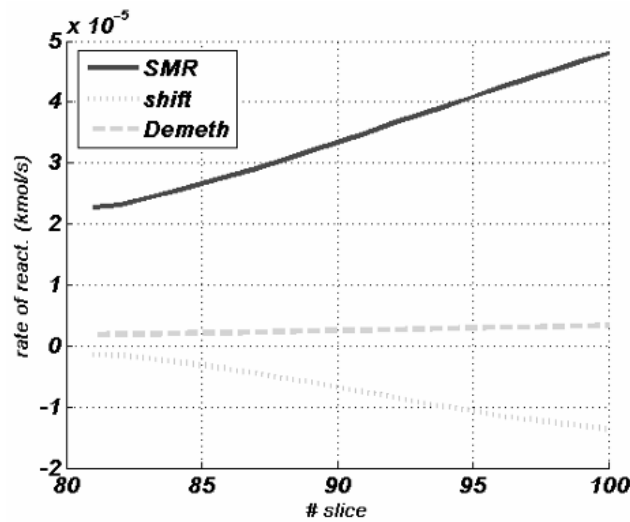


Figure 7. Pre-reformer reaction rates.

7.2 SOFC tube

Figure 8 shows that, in the first part of the SOFC tube, the reforming process is faster than the electrochemical one. Then, the reforming reactions reach very quickly to the equilibrium conditions (rates of reaction asymptotically approaching zero), whereas the electrochemical reaction continues to occur, depending on the shape of the polarization curve. Obviously, higher the cell operating voltage, lower the corresponding current density, i.e.: slower the electrochemical process. Conversely, the rates of the reforming reactions are basically related to the temperature and partial pressure fields.

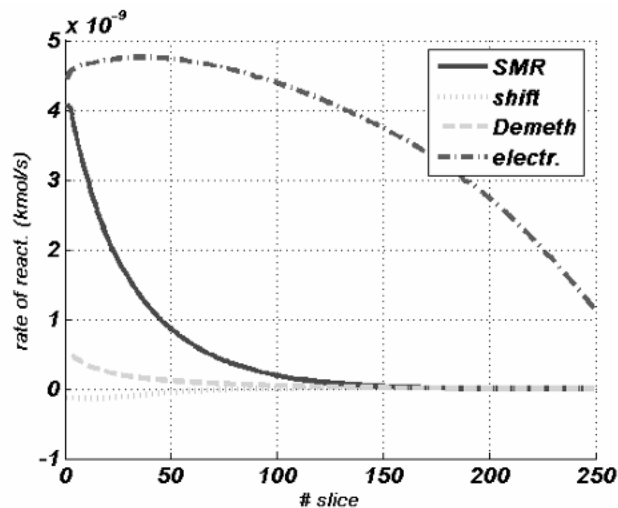


Figure 8. SOFC reaction rates.

The profile achieved in Figure 8 is much more detailed than those typically returned by 0-D models. In fact, in this case the calculation of chemical/electrochemical reaction rates is related to the local thermodynamic properties, whereas, in 0-D models, average values of the thermodynamic properties must be used (Calise et al., 2006 c). The rates of the four reactions (Gallucci et al., 2004) affect the trend

of the heat produced by the overall chemical-electrochemical process (Figure 9). In fact, at first, the reforming reaction is faster than the electrochemical one. Consequently, the heat generated by the hydrogen electrochemical oxidation is lower than that required by the reforming reactions. Then, the heat generated by the electrochemical reaction is much larger than that required by the internal reforming. Finally, in the last sections of the tube, the overall generated heat decreases, as a consequence of the reduction of the electrochemical rate of reaction. Furthermore, the shape of the current density function, displayed in Figure 10, is strictly related to the hydrogen availability, since the open circuit reversible voltage, and the activation and concentration overvoltages mainly depend on the hydrogen partial pressure. The SOFC under investigation is dramatically affected by the ohmic polarization.

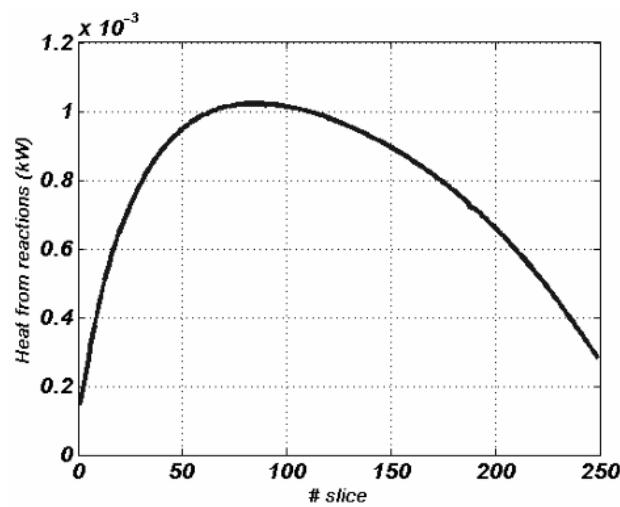


Figure 9. SOFC heat from reactions.

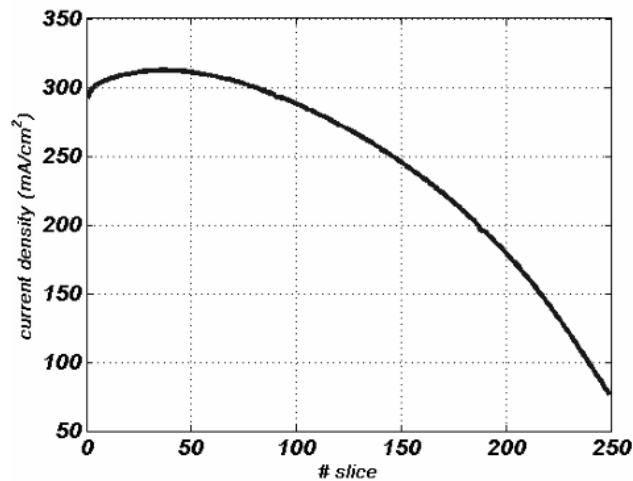


Figure 10. Current density.

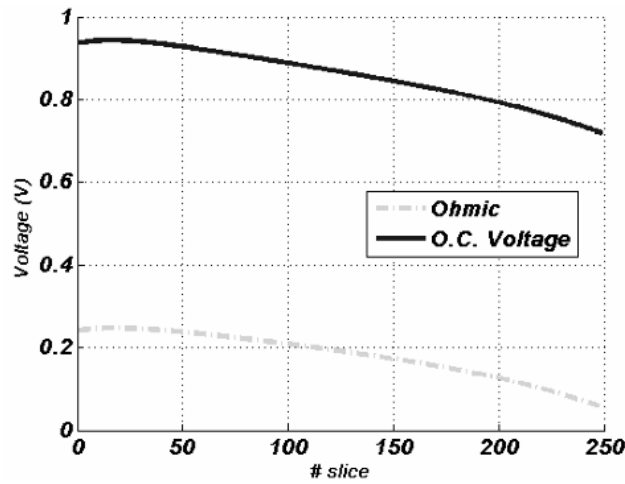


Figure 11. Nernst potential and Ohmic Overvoltage.

Figure 11 clearly shows that the Ohmic overvoltage is much higher than all other losses. The trend of the ohmic polarization curve reproduces the shape of the solid temperature (Figure 13). In fact, the higher the slice temperature, the lower the corresponding ohmic polarization. On the other hand, Figure 11 also shows the shape of the Nernst open circuit reversible voltage, dramatically depending on hydrogen, oxygen and water partial pressures. Thus, Nernst potential decreases since: H_2 and O_2 partial pressures decrease since those components are consumed by the electrochemical reaction whereas H_2O partial pressure increases since it is produced by the electrochemical reaction. Figure 12 shows the activation and concentration overvoltages in the SOFC tube. At first, the magnitude of the concentration overvoltage is much lower than the other polarizations. In addition, the cathodic concentration overvoltage is predominant on the anodic one. The trend of concentration overvoltage at the cathode is due to the shape of the current density displayed in Figure 10. Finally, the shape of the activation overvoltage is basically due to the solid temperature, displayed in Figure 13. In fact, the higher the operating temperature, the lower the corresponding activation overvoltage. In this case, this phenomenon is dominant over the reduction of hydrogen and oxygen partial pressures.

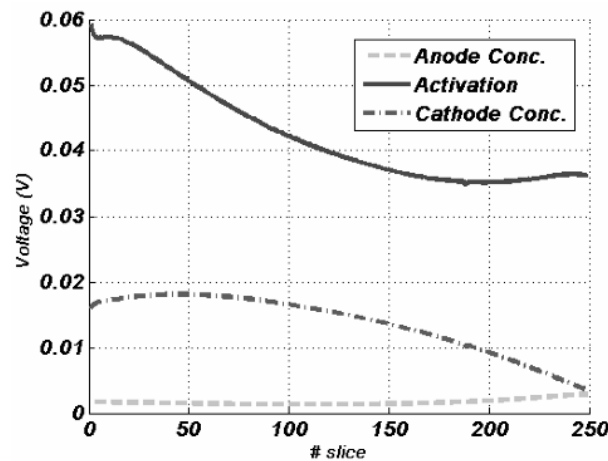


Figure 12. Concentration and activation overvoltages.

The result of the calculation of temperature fields is shown in Figure 13, as above discussed. The air enters the injection tube (slice 250, air injection stream), where it is preheated up to 942 °C (slice 1). Then, the air passes through the cathode compartment, with a change in the flow direction (slice 1, air cathode stream), exiting the cell at 968 °C (slice 250). On the other side, the temperatures of fuel inlet (slice 1, fuel stream) and outlet (slice 250, fuel stream) are 921 °C and 973 °C, respectively. So, the typical simplification of assuming the same temperature value for air and fuel outlet streams is not completely justified. In addition, Figure 13 shows that the SOFC cannot be considered isothermal, as usually assumed by a number of authors in simplified 0-D models.

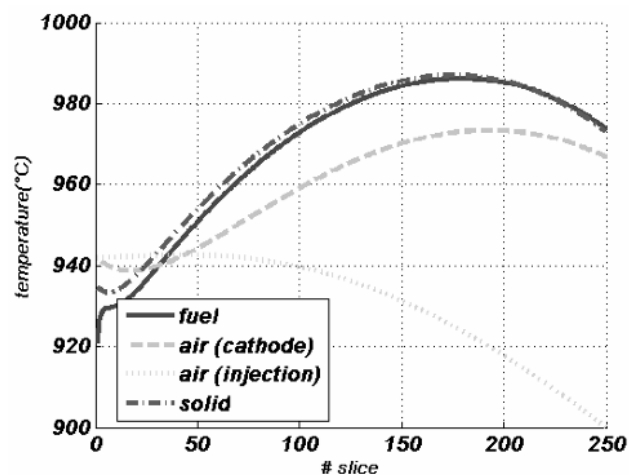


Figure 13. SOFC temperatures.

Moreover, the optimum temperature profiles, displayed in Figure 13, were achieved by handling the following parameters: pre-reformer demethanization rate, air to fuel ratio, air and fuel inlet temperatures, cell and injection tube diameters. Temperature curves are also influenced by the air to fuel ratio. In fact, the air mass flow rate is much higher than the stoichiometric value, in order to provide the appropriate stack cooling. Such cooling could also be achieved by lowering the air inlet temperature. However, in this case, remarkable temperature gradients along the SOFC tube axis would be achieved. All pressure drops in are low, and can be neglected. In particular, a slight pressure drop is perceptible only for the cathodic stream, as a consequence of the high mass flow rate and velocity.

Finally, Figure 14 shows the fuel molar flow rates along the SOFC axis, also putting in evidence the trend of the chemical and electrochemical phenomena occurring in the SOFC tube. In fact, in the first part of the SOFC the internal steam reforming process is dominant over the electrochemical reaction, inducing an increase of the hydrogen partial pressure. Conversely, in the same section the steam partial pressure decreases, because the amount of water used by the internal reforming process is much higher than the one released by the electrochemical process. Then, the steam reforming reactions quickly

approach the equilibrium conditions, as clearly shown in Figure 14, since CO, CO₂, CH₄ curves are flattening. In particular, the methane molar flow rate approaches the value of 0 kmol/s from the 20th slice of the control volume. This result shows that the high operating temperatures of the SOFC and its chemical and geometrical peculiarities permit to consume all the inlet methane within the cell. Conversely, the partial pressures of H₂ and H₂O decrease and increase, respectively, as a consequence of the progress of the electrochemical reaction.

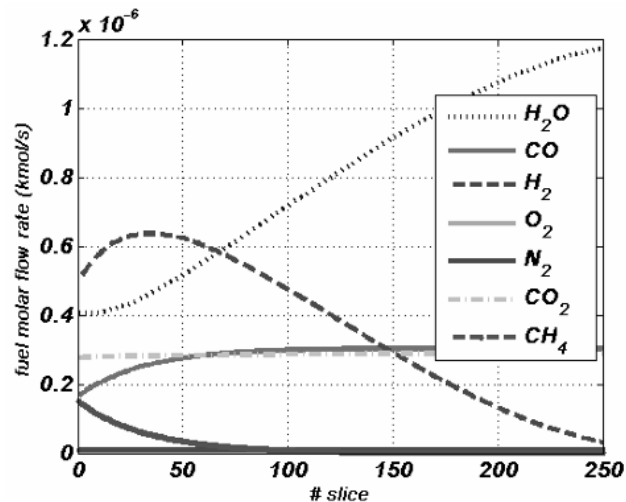


Figure 14. SOFC fuel molar flow rates.

The cell under investigation also shows a good chemical design. In fact, the overall fuel utilization factor approaches the value of 81 % accordingly with manufacturer requirements (Singhal et al., 2003). In fact, higher fuel utilization factor would need much higher cell active area, dramatically increasing SOFC capital costs. Obviously, the unreacted fuels can be usefully used in a combustor to provide the heat required to preheat inlet air and fuel streams

8. Conclusion

This paper presents an original approach for the finite-volume axial-symmetric simulation of a tubular SOFC. The simulation model presented allows accurate calculation of the main physical, chemical, electrical and electrochemical properties in the system, such as temperature, pressure, chemical composition, overvoltages, current, etc. Such approach includes a number of detailed models for the calculation of electrochemistry and of the kinetics of the internal reforming process, that were properly calibrated in order to comply with the SOFC experimental data (Calise et al., 2006 c). The results showed that some of the simplifying assumptions usually adopted in SOFC simulations are not rigorously acceptable, e.g.: the generator is not isothermal, concentration overvoltages cannot be considered negligible for whatever operating condition, the shift reaction is not equilibrium-controlled,

etc. The computer code presented in the paper will be the basis for more detailed analysis of the SOFC tube and of the stack in general, such as simulation of a complete stack and of hybrid plants and thermo-economic optimizations of the stack.

Nomenclature

V	Cell Voltage (V)
g_f	Gibbs free energy (kJ/kmol)
F	Faraday constant
R	Gas constant (kJ/kmol K)
p	Partial pressure (bar)
h	Overtoltage (V)
d	Thickness (m)
L	Length (m)
i	Current density (mA/cm ²)
D_{AB}	Binary diffusion coefficient
M	Molar mass (g/mol)
e	Porosity
x	Tortuosity
W_D	Lennard-Jones intercollision integral
s_{AB}	Lennard-Jones characteristic length (Å)
r_B	Bulk density (kg/m ³)
S_A	Pore area (m ²)

References

- Calise F., Dentice d'Accadia M., Palombo A., Vanoli L., 2006, *Simulation and exergy analysis of a SOFC-gas turbine system*, *Energy: the international Journal*, Volume: 31, Issue: 15, December, 2006, pp. 3278-3299
- Calise F., Palombo A., Vanoli L., 2006, *Design and partial load exergy analysis of a hybrid sofcgt power plant*, *Journal of power sources*, Volume: 158, Issue: 1, July 14, 2006, pp. 225-244
- Spakovsky M.R., 2006, *Single-Level Strategy for the optimal Sintheses/design of a Hybrid SOFCGT Power Plant*, *Journal of Power Sources*, Volume: 159, Issue: 2, September 22, 2006, pp. 1169-1185
- Calise F., Dentice d'Accadia M., Palombo A., Vanoli L., Vanoli R., 2004, *Modelling, simulation and exergy analysis of a hybrid SOFC -Gas Turbine System*. 3rd International Symposium Energy and environment 2004, Sorrento, 30th September to 2nd October.
- Campanari S., Iora P., 2004, *Definition and sensitivity analysis of a finite volume SOFC model for a tubular cell geometry*, *Journal of Power Sources* 132 (2004) 113—226

-
-
- Chan, S. H., Low, C. F., Ding, O. L., 2002, *Energy and exergy analysis of a simple solid – oxide fuel cell power system.*, *Journal of Power Sources*, vol. 103, pp.188-200.
- Chan, S.H., Ho, H.K., Tian, Y., 2003, *Multi-level modelling of SOFC-gas turbine Hybrid system*, *International Journal of Hydrogen Energy* 28 (2003) 889-900.
- Chan S.H., Kior K.A., Xia, Z.T., 2001, *a complete polarization model of a solid oxide fuel cell and its sensitivity to the change of cell component thickness*, *Journal of Power Sources* 93 (2001) 130-140
- Costamagna, P., Magistri, L., Massardo, A., 2001, *Design and part-load performance of a hybrid system based on a solid oxid fuel cell reactor and a micro gas turbine*, *Journal of Power Sources* 96 (2001) 352-368.
- CEIC0010, *Diffusion vs Mass Transfer by Bulk Motion, Fick's Law and Mass transfer rate equation.*
- Fuel cell handbook (sixth edition)*, 2002, U.S. Departement of Energy.
- Gallucci, F., Paturzo, L., Basile, A., 2004, *A simulation study of the steam reforming of methane in a dense tubular membrane reactor*, *International Journal of Hydrogen Energy*, vol. 29, pp. 611 – 617.
- Larminie, J., Dicks, A., 2004, *Fuel cell system explained*, John Wiley & sons LTD.
- Nisancioglu, K., 1989, *Natural gas fuelled solid oxide fuel cells and systems, ohmic losses*, *Workshop on mathematical modelling*, Charmey/Switzerland, july 2 to 6 1989.
- Reid, Prausnitz, *The Properties of gases and liquids*, Mc Graw Hill, 1977
- Stiller, C., Thorud, B., Seljebo, S., Mathisen, O., Karoliussen, H., Bolland, O., 2005, *Finite volume modelling and hybrid-cycle performance of planar and tubular solid oxide fuel cells*, *Journal of Power Sources* 141 (2005) 227-240.
- Singhal, S.C., Kendall, K., 2003, *High temperature Solid Oxide Fuel Cells*, Elsevier.
- Todd B., Young J.B., 2002, *Thermodynamic and transport properties of gases for use in solid oxide fuel cell*, *Journal of power Sources* 110 (2002) 186-200
- Xu, J., Froment, G. F., 1989, *Methanes-steam reforming: methanation and water-gas shift: I. Intrinsic kinetics*, *AIChE Journal*, vol.35 no.1.
- Chemical Properties Handbook*, 1999, McGraw Hill, pp. 531-556.

Design of Evaporation Systems and Heaters Networks in Sugar Cane Factories Using a Thermoeconomic Optimization Procedure*

Adriano V. Ensinas**; Silvia A. Nebra

Mechanical Engineering Faculty, State University of Campinas, Cidade Universitária
Zeferino Vaz, Campinas-SP, Brazil, P.O. Box: 6122. e-mail:
adrianov@fem.unicamp.br

Miguel A. Lozano; Luis Serra

Mechanical Engineering Department, University of Zaragoza,
CPS de Ingenieros, C/ Maria de Luna 3, Zaragoza, Spain, 50018.

ABSTRACT

Sugar cane production in Brazil is one of the most competitive segments of the national economy, producing sugar and ethanol for internal and external markets. Sugar production is done basically in several steps: juice extraction, juice clarification and evaporation, syrup treatment and sugar boiling, crystallization, centrifugation and drying. Much heat exchange equipment is used in this process.. An optimized design of the evaporation system with the correct distribution of the vapor bleed to attend other parts of the process may contribute to exhausted steam demand reduction. This paper presents a thermoeconomic optimization of the evaporation system and the heaters network of a sugar factory, aiming at minimum investments and operation costs. Data from Brazilian sugar factories were used to define the process parameters. The methodology proposed is used to evaluate the cost of the steam consumed by the factory and the optimized design of the equipment.

Keywords: Sugar cane, sugar process, thermoeconomic optimization, heat recovery, process

1. Introduction

Sugar and ethanol production from sugar cane in Brazil is one of the most competitive sectors of the national economy. The bagasse generated by the productive process is used as fuel in cogeneration systems that offer thermal and electrical energy to the process. In the last few years many sugar cane factories have been producing a surplus of electricity that may be sold for the grid, becoming a new product.

Currently there are more than 300 cane factories operating all around the country (UNICA, 2006). These units crushed more than 394.4 MT of cane in the 2005/2006 harvest season, with a total production of more than 26.7 MT of sugar and 17.0 Mm³ of ethanol (CONAB, 2006).

Sugar production is basically done in several steps: juice extraction, clarification and evaporation, followed by syrup treatment and sugar boiling, crystallization, centrifugation and drying. Heat requirements of the process occur mainly in the evaporation system and the sugar boiling step, but heaters of the extraction system, juice and syrup treatments also consume important amounts of heat.

The reduction of exhausted steam demand by the production process may increase the surplus of electricity generated by the cogeneration system, but its feasibility must be evaluated considering investment costs. From an economic point of view, the prices paid for the surplus of electricity generated and the investments necessary for new heat exchange equipment determine the feasibility of the exhausted steam demand reduction. A thermoeconomic optimization can indicate the most adequate investment.

The purpose of this paper is to perform a thermoeconomic optimization of the evaporation system and heaters network design, analyzing for the optimized distribution of the vapor bleed and the heat transfer area necessary for each piece of equipment.

Data of sugar process parameters used for the process simulation were obtained from sugar cane factories in Brazil.

2. Sugar process description

The sugar production from sugar cane is basically done by the following steps depicted in Figure 1:

- Juice Extraction System (I): sugar cane bagasse and juice are separated. Traditional sugar factories use mills where juice is extracted by compression. Diffusers can also be used, extracting raw juice by a process of lixiviation, using for that imbibitions hot water and recirculation of the juice extracted. Both systems require previous cane preparation, done using knives and shredders that operate with direct drive steam turbines. The plant studied in this paper operates with a diffuser that demands thermal energy for the heating of the recirculating juice.

The sugar cane bagasse produced at the extraction is delivered to the cogeneration system, where it is used as fuel, producing the electricity and steam consumed by the process.

- Juice Clarification (II): some non-sugar impurities are separated by the addition of some chemical reactants as sulfur, lime, among others. Juice heating is necessary for the purification reactions. After heated, the juice passes through a flash tank, before entering the clarifier.

- Juice Evaporation (III): juice is concentrated in a multiple-effect evaporator. Exhausted steam from the cogeneration system is used as thermal energy source in the first evaporation effect, which separates an amount of the water presented in the juice, and so producing, the heating steam for the next evaporation effect. The system works with decreasing pressure due to a vacuum imposed in the last effect, to produce the difference of temperature between each effect. The vapor generated in each effect may be used to attend other heat requirements of the process.
- Syrup Treatment (IV): syrup (concentrated juice) from the evaporation system is purified to improve the quality of the final product. Firstly the syrup is heated and then a flotation of the impurities is done with addition of some chemical reactants.
- Sugar Boiling, Crystallization and Centrifugal Separation (V): syrup is boiled in vacuum pans for crystal formation and then directed to crystallizers to complete crystal enlargement. After that, the sugar crystals formed are separated from molasses in centrifugals.
- Sugar Drying (VI): sugar is dried to reduce its moisture content in order to be stored.
- Cogeneration System (VII): Steam and electricity are produced to attend process demand. Usually sugar cane bagasse is used as fuel for boilers that produce high pressure steam to move back-pressure or extractioncondensation turbines in a steam cycle.

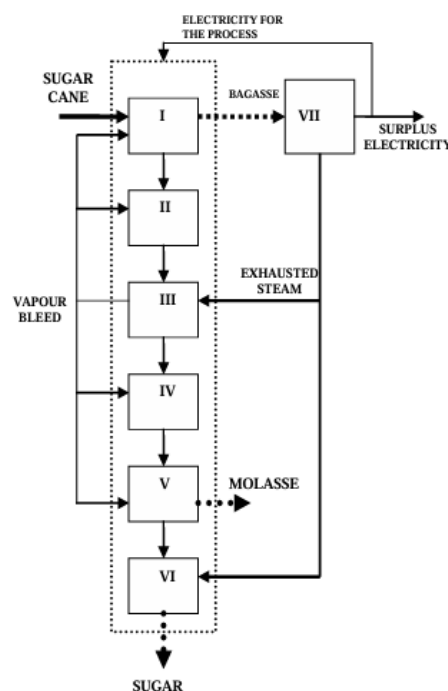


Figure 1. Scheme of a sugar factory with the cogeneration system.

3. Thermoeconomic optimization procedure

The thermoeconomic optimization procedure was performed using the EES software (EES, 2006), aiming at the optimum design of the evaporation system and the heaters network with a minimum total cost including operation costs (heating steam cost) and investments costs (equipment). The final cost results were based in a sugar factory that crushes 10,000 t cane/year. The reference environment presented by Szargut (1988) was used for the determination of the exergy of sugar cane, bagasse, steam and condensates.

A base case was defined that represents the current design found in Brazilian sugar factories, and used for the comparison of the results obtained after the optimization procedure.

The optimization was performed, dividing the plant into sub-systems that could be optimized separately in an iterative procedure with satisfactory results (Lozano et al., 1996). Four sub-systems listed below were optimized:

A. Extraction system

B. Juice clarification

C. Syrup treatment

D. Evaporation system

For the heaters that were designed in subsystems A, B and C, the decision variable was the juice/syrup outlet temperature in each heater ($t_{j,out}$), and for the evaporation system (D) the saturation temperature of the steam generated at the evaporation effects ($t_{w,sat}$).

Figure 2 shows the adopted steps of the optimization procedure.

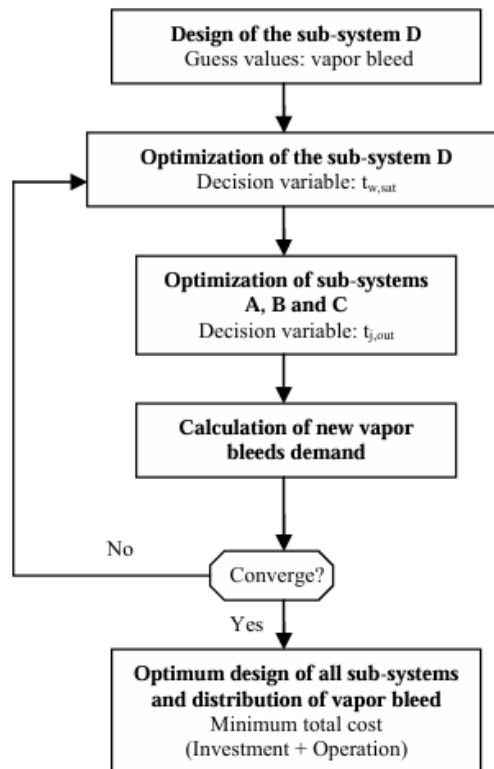


Figure 2. Iterative optimization procedure steps.

Other parameters listed below were calculated, defining an optimized design of the equipment with the minimum total cost.

For the heaters network the following parameters were defined:

- Number of heating stages;
- Heating requirements;
- Logarithmic mean temperature difference;
- Heat transfer area;
- Investment cost;
- Monetary cost of heating steam consumed.

And for the evaporator system the following parameters were defined:

- Operation pressure of evaporators;
- Juice boiling point elevation;
- Temperature of boiling juice;
- Intermediate juice concentration;

- Heat transfer area;
- Investment cost;
- Monetary cost of heating steam consumed;
- Monetary cost of vapor bleed and condensates produced.

The objective function, for the evaporation system and the heaters network, were defined by Equations 1 and 2 respectively.

Equation 1 minimizes the total cost of the evaporation system including investment cost of the heat transfer area in each evaporator (Z_e). The operation cost considers and the heating steam cost in the first effect of evaporation (C_s) and as products, which reduce the total cost of this subsystem, the vapor bleeds (C_v) and useful condensates costs (C_c).

For the heaters network, the objective function, defined by Equation 2, includes the investment cost of the heat transfer area in each heater and operation cost which considers the cost heating steam (C_s) and the useful condensate (C_c).

$$MinC_{evap} = \sum_e Z_e + \sum_s C_s - \sum_v C_v - \sum_c C_c \quad (1)$$

$$MinC_{he} = \sum_e Z_e + \sum_s C_s - \sum_c C_c \quad (2)$$

The total cost of the plant is defined by Equation 3, which considers the sum of minimum cost of all subsystems obtained after the procedure of optimization.

$$C_{tot} = \sum_n C_n \quad (3)$$

3.1. Economic model

3.1.1. Determination of the steam cost

The cost of each stream of steam demanded by the process was estimated using the theory of exergetic cost (Lozano and Valero, 1993).

Firstly, exergy of the bagasse and sugar cane was calculated. For the determination of bagasse exergy, a methodology presented by Sosa-Arnan and Nebra (2005) was adopted. The referred methodology is a variation of one proposed by Szargut et al. (1988) for wood, with the necessary changes in the composition and low heat value of the fuel. For the bagasse at the reference environment conditions, its total exergy is equal to its chemical exergy. The following composition of the bagasse in mass and dry base was assumed: C(47.0%), H(6.5%), O(44.0%) and Ash(2.5%) (Baloh and Wittner, 1990). The

exergy of the sugar cane was obtained with the sum of the bagasse exergy and the juice exergy calculated following procedures for sucrose-water solutions presented by Nebra and Fernández-Parra (2005).

Thus, for a determined production cost of the sugar cane ready to be processed, the monetary cost per unit of exergy (c) of the sugar cane could be calculated as follows:

$$c_{cane} = \frac{C_{cane}}{m_{cane} ex_{cane}} \quad (4)$$

The “ c ” of the bagasse used as fuel at the cogeneration system was assumed to be the same as the sugar cane that enters the factory at the extraction system.

$$c_{cane} = c_{bag} \quad (5)$$

So, the live steam produced by the boiler at the cogeneration system had its “ c ” obtained using Equation 6.

$$c_s = \frac{(c_{bag} \dot{m}_{bag} ex_{bag}) + Z_{bl}}{\dot{m}_s (ex_s - ex_w)} \quad (6)$$

The exhausted steam from the back pressure steam turbine of the cogeneration and the vapor generated in the evaporators were considered alternatives of heating sources to the process. So, to perform the optimization, it was assumed as a hypothesis, that they have the same “ c ” of the live steam. The “ c ” of condensates generated after the steam condensation at the heat exchangers are also the same.

So, the monetary cost (C) of each steam stream could be calculated multiplying its “ c ” by its total exergy (Equation 7). TABLE I shows the parameters adopted for the determination of the steam monetary cost.

$$C_s = c_s \dot{m}_s ex_s \quad (7)$$

TABLE I. DATA FOR DETERMINATION OF
STEAM COST.

Parameter	Value
Boiler capital cost (10^6 US\$) ¹	12
Sugarcane production cost (US\$/t) ²	14
Available bagasse (kg/t cane) ³	252
Live steam pressure (bar)	63
Live steam temperature (°C)	480
Boiler feed water temperature (°C)	122
Boiler efficiency (%) ⁴	85

1 cost of boiler with following characteristics: 63 bar, 480°C, 200 t of steam/h including costs of installation and instrumentation (Dedini, 2006).

2 cost of sugar cane ready to be processed at the State of Sao Paulo, Brazil in 2006 (Usina Santa Isabel, 2006).

3 wet base (50% of moisture)

4 LHV base

3.1.2. Determination of investment costs

The investment cost of evaporators and heaters could be calculated using Equations 8 to 10. Scaling exponent is used to correct the reference equipment purchase cost for the optimized heat transfer area (Equation 9) (Bejan et al., 1996). Data used are shown in TABLE II.

$$\dot{Z}_e = E_e \xi \quad (8)$$

where:

$$E_e = E_r \left(\frac{A_e}{A_r} \right)^\alpha \quad (9)$$

$$\xi = \frac{i(1+i)^j}{(1+i)^j - 1} \quad (10)$$

TABLE II. DATA FOR DETERMINATION OF EQUIPMENT COST.

Parameter	Value
Evaporator purchase cost (10^3 US\$) ¹	476
Heater purchase cost (10^3 US\$) ²	43
Evaporator scaling factor ³	0.7
Heater scaling factor ³	0.5
Annual interest rate (%)	10
Equipment useful life (years)	15
Factory operation hours per year	4000

1 cost of installed evaporator Robert type with 4000m² of area (Usina Santa Isabel, 2006).

2 cost of installed carbon steel shell and tube juice heater with 300m² of area (Usina Santa Isabel, 2006).

3 Source: Chauvel et al., 2001.

A maximum heat transfer area was adopted for evaporators or heaters to represent a realistic design of

the equipment. The maximum size of an evaporator was admitted as 5000m² and for heaters this limit was 1000m². If the optimization indicates that an equipment size is bigger than these values, the procedure divides the total area, showing some equipment in parallel which attends the limits imposed.

3.2. Physical model

3.2.1. Evaporation system

The developed evaporation system model uses Robert type five-effect evaporators, which operate with a vacuum at the last effect, producing the difference of temperature between each effect. Some restrictions are imposed for the optimization:

- Juice enters at 15% of solid content and leaves at 65%.
- Maximum temperature of 115°C for juice boiling at the first effect to avoid juice sucrose loss and coloration (Baloh and Wittner, 1990).
- Minimal pressure of 0.16 bar at the last effect (Hugot, 1986).
- 5% of heat loss (Hugot, 1986).

A heat demand of sugar boiling system was estimated as 98 kWh/t cane, and it was assumed that it is attended by the vapor produced in the first effect of evaporation. Sugar drying heat was estimated as 5 kWh/t cane is provided by the exhausted steam from the cogeneration system.

The enthalpy of the juice was calculated using Equation 11 (Kadlec, 1981):

$$h_j = (4.1868 - 0.0297x_j + 4.6E^{-5}x_jPu_j)t_j + 3.75E^{-5}x_jt_j^2 \quad (11)$$

The temperature of evaporation (Equation 12) in each effect is defined as the sum of the temperature of saturation of pure water at the vapor space for a given operation pressure and the boiling point elevation due the concentration of the juice (Peacock (1995) (Equation 13). The effect of the boiling point elevation due the hydrostatic effect of liquid column was neglected.

$$t_{\text{evap}} = t_{w,\text{sat}} + \Delta t_{\text{bpe}} \quad (12)$$

$$\Delta t_{\text{bpe}} = 6,064E^{-5} \left[\frac{(273 + t_{w,\text{sat}})^2 x_{j,\text{out}}^2}{(374,3 - t_{w,\text{sat}})^{0,38}} \right] + (5,84E^{-7} (x_{j,\text{out}} - 40)^2 + 0,00072) \quad (13)$$

3.2.2. Heaters network

The heaters network includes sub-systems A, B and C previously indicated.

Data of each sub-systems are presented in TABLE III. The purity of the heated flow is considered constant at 85% and 5% of heat loss is considered for each heater (Hugot, 1986).

TABLE III. DATA OF SUB-SYSTEMS

A, B AND C.					
Sub-System	\dot{m}_j (kg/s)	x_j (%)	$t_{j,in}$ (°C)	$t_{j,out}$ (°C)	
A Extraction System ¹	124.8	15	80.0	92.0	
B Juice Clarification	124.8	15	62.0	105.0	
C Syrup Treatment	28.8	65	Evaporator outlet	80.0	

¹ this sub-system is composed by a diffuser with re-circulation of the raw juice in 3 heating stages (Usina Cruz Alta, 2005).

3.2.3. Heat transfer area

The heat transfer area defines the investment cost of evaporators and heaters, and can be calculated by Equation 14.

$$A = \frac{Q}{U\Delta t} \quad (14)$$

Equations 15 (Van der Poel et al., 1998) and 16 (Hugot, 1986) were used to calculate the heat exchange coefficients of evaporators and heaters respectively. The juice velocity circulation at the heaters was assumed constant at 1.5 m/s.

$$\Delta t_{evap} = t_{s,in} - t_{evap} \quad (17)$$

$$\Delta t_{he} = \frac{(t_s - t_{j,in}) - (t_s - t_{j,out})}{\ln\left(\frac{t_s - t_{j,in}}{t_s - t_{j,out}}\right)} \quad (18)$$

For the determination of the difference of temperature (Δt) in the evaporators and heaters, Equations 17 (Hugot, 1986) and 18 were used respectively.

$$\Delta t_{evap} = t_{s,in} - t_{evap} \quad (17)$$

$$\Delta t_{he} = \frac{(t_s - t_{j,in}) - (t_s - t_{j,out})}{\ln\left(\frac{t_s - t_{j,in}}{t_s - t_{j,out}}\right)} \quad (18)$$

3.3. Base case

A base case is assumed to compare and validate the results of the optimization procedure. The evaporation system is composed by a Robert type five-effect evaporator working at the following

pressure in each effect: 1.69, 1.07, 0.76, 0.46, 0.16 bar of absolute pressure (Usina Cruz Alta, 2005)

As it occurs in many sugar factories in Brazil, for this base case, there is not a thermal integration of the process and all the juice and syrup heaters of the factory consume vapor from the first effect of evaporation that attends the heat demand of sugar boiling system too. So, sub-systems a, b and c have only one heater as shown in Figure 3

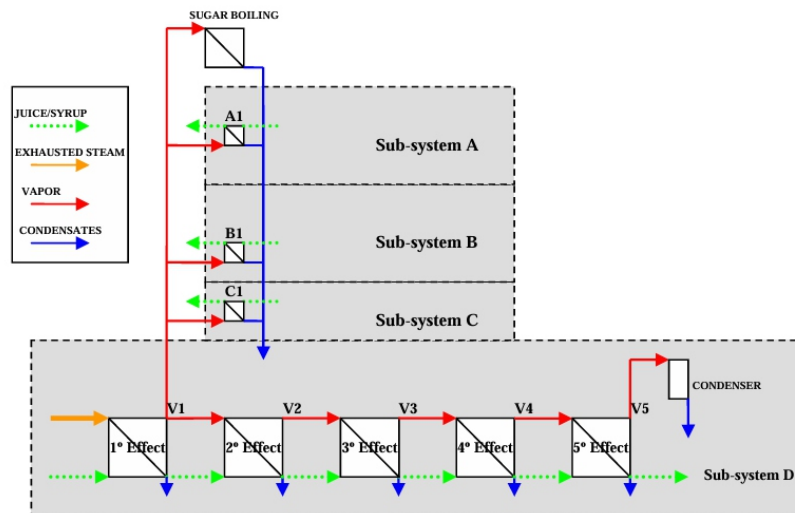


Figure 3. Lay-out of the base case.

4. Results

Using the optimization procedure described above, the optimum design of the evaporation system and heaters network of the sugar factory could be determined. TABLE IV shows the monetary costs per unit of exergy calculated for the sugar cane and live steam that were used for the calculation of the operation costs, once determines the costs of heating steam and condensates as previously explained.

TABLE IV. MONETARY COSTS PER UNIT
OF EXERGY.

Monetary cost per unit of exergy (10 ⁻⁶ US\$/kJ)	
Sugar Cane	2.788
Steam	10.864

Figure 4 shows the lay-out of the equipment optimized at the factory. In this figure the proposed sub-systems can be seen, including also the distribution of the vapor bleeding from the evaporator. The detailed parameters of each heater are shown in TABLE V.

TABLE V. OPTIMIZED HEATERS
NETWORK.

	Area (m ²)	Heating Steam Consumed ¹	Heating Steam Flow Rate (kg/s)	T _{j,in} (°C)	T _{j,out} (°C)
A1	1000	V4	1.76	80.0	87.9
A2	1000	V4	1.76	80.0	87.9
A3	1000	V4	1.76	80.0	87.9
A4	265	V3	0.94	87.9	92.0
A5	265	V3	0.94	87.9	92.0
A6	265	V3	0.94	87.9	92.0
B1	1000	V4	5.92	62.0	88.5
B2	1000	V4	5.92	62.0	88.5
B3	994	V3	2.30	88.5	98.6
B4	749	V2	1.48	98.6	105.0
C1	162	V4	0.82	58.3	80.0

¹ “V” denotes vapor bleed and the “number”, the evaporation effect it was produced.

As seen in TABLE V, after the thermoeconomic optimization a certain distribution of the vapor produced by the evaporation system was obtained. The new layout promotes a better use of each evaporation effect vapor bleed, contributing for a higher thermal integration of the factory, with a minimal cost

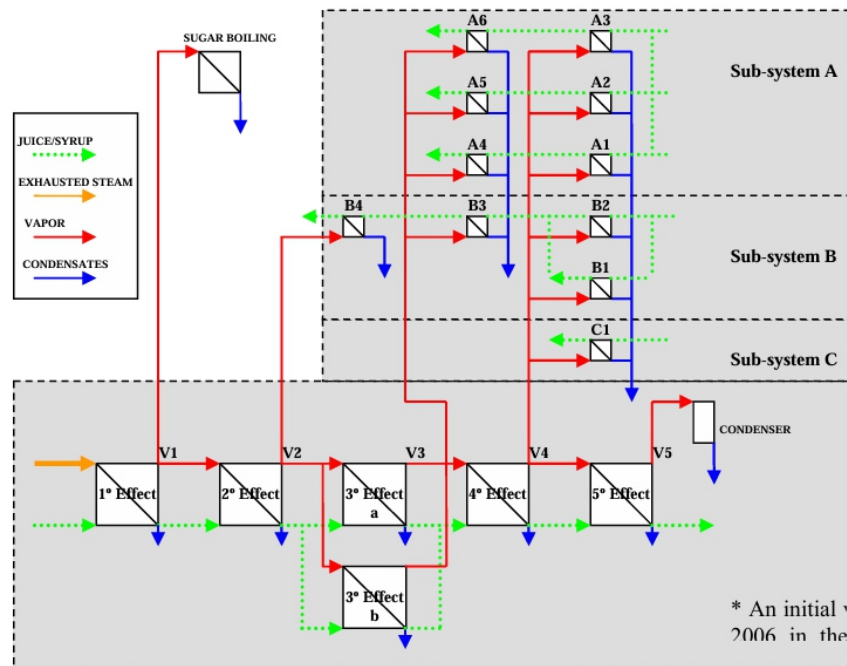


Figure 4. Lay-out of the optimized case.

The higher cost of the exhausted steam from the cogeneration system limits its use as a heating source for the heaters in an optimized design. The available vapor bleeds have adequate temperatures for the heating requirements, reducing the total cost of these sub-systems. The consumption of exhausted steam from the cogeneration system decreased when compared with the base case (TABLE VI). As expected, the use of vapor bleeds from the last evaporation effects, substituting vapor bleed from the first one, promoted the reduction of steam requirements of the evaporation system, that could evaporate the same amount of water using 16% less energy.

TABLE VI. EXHAUSTED STEAM DEMAND.

	Exhausted Steam Demand ¹ (kg/t cane)
Base Case	490
Optimized Case	412

¹saturated at 2.5 bar of pressure

The evaporation system was designed to have the minimum cost at the optimized case, as its parameters are those presented in TABLE VII.

TABLE VII. OPTIMIZED EVAPORATION
SYSTEM DESIGN.

Effect	Area (m ²)	p (bar)	t _{w,sat} (°C)	Δt _{bpe} (°C)	t _{evap} (°C)
1°	3324	1.69	115.0	0.5	115.5
2°	4808	1.38	109.0	0.7	109.7
3°a	3615	1.12	102.9	1.3	104.2
3°b	3615	1.12	102.9	1.3	104.2
4°	5000	0.75	91.9	3.1	95.0
5°	246	0.16	55.0	3.3	58.3

The final results for base and optimized cases in each sub-system can be seen in TABLES VIII and IX respectively.

TABLE VIII. COSTS FOR THE BASE CASE.

Sub-system	Investmen t (US\$/h)	Operation ¹ (US\$/h)	Total (US\$/h)
------------	-------------------------	------------------------------------	-----------------------

Extraction System	4.3	167.1	171.4
Juice Clarification	4.7	199.4	204.1
Syrup Treatment	0.5	17.0	17.5
Evaporator	62.9	334.3	397.1
TOTAL	72.3	717.7	790.1

1 Operation cost considers the cost of heating steam and the reduction cost due the production of vapor and/or condensates that are used in other parts of the factory.

As can be seen in TABLES VIII and IX, after the thermoeconomic optimization was performed, a reduction of the total cost was obtained in each sub-system when compared with the base case. The investment in equipment increased, as heating steam of a lower quality is used at the heaters, requiring bigger surfaces of heat exchange. On the other hand, the reduction of consumed steam cost compensates its investment in new heaters and the total cost decreases for each sub-system.

The use of vapor from the 1st, 2nd, 3rd and 4th effect of evaporation reduced the total cost of all sub-systems considerably, even increasing more than 50% the investment in new equipment.

The clarification, contributes with 13.5% of the total cost reduction. The extraction system reduced 10.9% of the total cost substituting the use of V1 in the base case for V3 and V4 in the optimized one. Syrup treatment contributed with 1.7% of the total reduction using V4.

TABLE IX. COSTS FOR THE OPTIMIZED CASE.

Sub-system	Investment (US\$/h)	Operation ¹ (US\$/h)	Total (US\$/h)
Extraction System	13.7	138.0	151.7
Juice Clarification	12.5	167.2	179.7
Syrup Treatment	0.9	13.4	14.3
Evaporator	82.6	181.2	263.8
TOTAL	109.6	499.8	609.5

1 Operation cost considers the cost of heating steam and the reduction cost due the production of vapor and/or condensates that are used in other parts of the factory.

The higher reduction of cost was obtained at the evaporation system with 33.6% of savings in this subsystem. This represents 73.8% of the total cost reduction obtained, showing the importance of the optimized design of this equipment for the sugar process cost reduction.

5. Conclusions

The thermoeconomic optimization presented in this paper showed to be very useful in analyzing the cost generation when designing a heaters network and evaporation system of a sugar factory, aiming at minimum investment and operation costs, and so choosing an alternative for thermal integration of the factory. The evaporation system represents the largest part of the total cost of the factory in thermal energy consumption. Its investment cost is substantially higher than the heaters, showing the importance of its optimized design. Moreover it produces the heating source for the other subsystems, influencing their designs too.

The optimization of the thermal energy consumption in sugar factories can also be important for evaluating the cost of exhausted steam demand reduction. The decision of the best technology to be implemented in the cogeneration system depends on the quantity of steam consumed by the process. The analysis of both systems must be made together aiming at the best alternative for the factory as a whole.

Acknowledgements

The authors would like to acknowledge Usina Cruz Alta, Guarani and Santa Isabel engineers, technicians and managers for available process data and FAPESP, CAPES and CNPq for the financial support to do this study.

Nomenclature

A	Heat transfer area (m ²)
ex	Specific exergy (kJ/kg)
c	Monetary cost per unit of exergy (US\$/kJ)
C	Monetary cost (US\$/s)

E	Equipment purchase cost (US\$)
h	Specific enthalpy (kJ/kg)
i	Annual interest rate (%)
j	Equipment useful life (years)
\dot{m}	Mass flow rate (kg/s)
p	Pressure (bar)
Pu	Purity (%)
Q	Heat power (kW)
t	Temperature (°C)
U	Heat exchange coefficient (kW/m ² K)
x	Solid content (%)
Z	Equipment cost (US\$/s)

Greek Letters

α	Scaling exponent
v	Velocity (m/s)
ξ	Amortization factor (s ⁻¹)
τ	Operation Hours (hours/year)

Subscripts

bag	bagasse
bl	boiler
bpe	boiling point elevation
c	useful condensate
cane	sugar cane
e	equipment
evap	evaporator
he	heater
in	inlet flow
j	juice/syrup
out	outlet flow
r	reference equipment
s	heating steam
sat	saturation
tot	total
v	vapor bleed
w	water

6. References

- Baloh, T., Wittwer, E., 1995, *Energy manual for sugar factories*. 2^o Ed. Verlag Dr. Albert Bartens. Berlin.
- Bejan, A., Tsatsaronis, G., Moran, M., 1996, *Thermal design optimisation*, John Wiley & Sons Inc, New York.
- Chauvel, A., Fournier, G., Raimbaut, C., 2001, *Manuel d'évaluation économique des procédés* Nouvelle Édition Revue et Augmentée. Editions Technip, Paris, France.
- CONAB - Companhia Nacional de Abastecimento, 2006, *Sugar cane harvest 2005/2006, December 2005*. Available at: <http://www.conab.gov.br> (In Portuguese)

-
-
- Dedini S/A Industrias de Base, 2006, Personal communication.*
- EES Engineering Equation Solver, F-Chart, 2006.*
- Hugot, E., 1986, Handbook of cane sugar engineering. 3rd Ed. Elsevier Publishing Company, Amsterdam.*
- Kadlec, P., Bretschneider, R., Dandar, A., 1981, The measurement and the calculation of the physical –chemical properties of water-sugar solutions, La Sucrierie Belge, Vol. 100, pp. 4559. (In French).*
- Lozano, M. A., Valero, A., 1993, “Theory of the exergetic Cost”, Energy. v.18. n°9. pp. 939-60.*
- Lozano, M.A., Valero, A., Serra, L., 1996, “Local optimization of energy systems”, Proceedings of the ASME 1996 Advanced Energy Systems Division. AES-Vol. 36. pp. 241250.*
- Nebra, S.A., Fernandez Parra, M.I., 2005. “The exergy of sucrose-water solutions: proposal of a calculation method”, Proceeding of ECOS 2005 – 18th International Conference on Efficiency, Cost, Optimization, Simulation and Environmental. Trondheim, Norway. 20-23 June 2005.*
- Peacock, Stephen, 1995, “Predicting physical properties of factory juices and syrups”, International Sugar Journal, Vol. 97, No. 1162, pp. 571–7.*
- Sosa-Arnao, J.H., Nebra, S. A., 2005, “Exergy of sugar cane bagasse”, Proceedings of 14th European Biomass Conference & Exhibition. Biomass for Energy, Industry and Climate Protection. 17-21 October 2005, Paris – France.*
- Szargut, J., Morris, D.R., Steward, F.R., 1988, Exergy analysis of thermal, chemical and metallurgical Processes. Hemisphere Publishing Corporation. New York, USA.*
- UNICA – União da Agroindústria Canavieira de São Paulo, 2006. Available at: <http://www.unica.com.br> (In Portuguese)*
- Usina Cruz Alta, 2005, Olímpia, SP-Brazil. Personal communication.*
- Usina Santa Isabel, 2006, Novo Horizonte, SP-Brazil. Personal communication.*
- Van der Poel, P.W. Schiweck, H. and Schwartz, T., 1998, Sugar Technology, beet and cane Sugar manufacture. Verlag Dr. Albert Bartens, Berlin*

From Watt's Steam Engine to the Unified Quantum Theory of Mechanics and Thermodynamics

George N. Hatsopoulos
Former Member of the Mechanical Engineering Faculty
and Member of the Corporation, Emeritus
Massachusetts Institute of Technology
77 Massachusetts Ave., Cambridge, MA 02139, USA
E-mail: gnh@pharosllc.com

ABSTRACT

Thermodynamics is the science that deals with all the phenomena that involve the transfer of energy, i.e. heat and work. Its development started in 1824 with the efforts of Sadi Carnot to improve the closed-cycle steam engine discovered by James Watt in 1764. In 1850, R. Clausius laid the foundations of the laws of thermodynamics. Soon thereafter a conflict between the second law of Thermodynamics and the laws of mechanics was pointed out by Maxwell in 1871 and was illustrated clearly by what has come to be known as Maxwell's demon. This conflict was addressed by Brillouin (1949) based on the work of Szilard (1929) and of many others. They all claimed that although the objective state of a system is fully describable by mechanics, classical or quantum, and evolves according to the laws of mechanics, some states of the system as perceived by an observer are subjective and reflect the lack of information the observer has about the actual mechanical state of the system. This point of view is, in effect, the information-theory interpretation of thermodynamics which, currently, is widely accepted. The central point of this paper is to describe the reasons why the information-theory interpretation of thermodynamics is contrary to physical reality. It shows that a logically viable hypothesis which reconciles mechanics with thermodynamics is the existence in nature of physical states that have objective uncertainties broader than those implied in quantum theory as it is traditionally formulated. The consequences of this hypothesis are presented in the Unified Quantum Theory of Mechanics and Thermodynamics, by Hatsopoulos and Gyftopoulos.

Keywords: Thermodynamics, Unified Quantum Theory of Mechanics and Thermodynamics, information-theory interpretation of thermodynamics, physical states with broader objective uncertainties, quantum theory

1. Thermodynamics

Thermodynamics is a physical science dealing with the transfer and the transformation of energy. Its development started in 1824 by Sadi Carnot, an engineer; more than a century after Isaac Newton established the foundations of classical mechanics. Ever since that time there has been, on and off, concerns expressed relating to conflicts between these two sciences.

The motivation behind Carnot's scientific effort was to find the basis of improving Watt's steam engine, invented 60 years earlier. Unlike steam engines in the past, Watt's engine was the first steam engine that did not consume water, it only received heat and produced work. Thus, it was the first true "Heat Engine". At that time the scientific community thought that heat was a fluid called caloric and that Watt's engine was nothing but a turbine that takes that fluid from a high level (a boiler at high temperature), produces useful work, and ejects it at a lower level (a condenser at lower temperature).

Carnot devised a reversible engine operating in a different cycle than Watt's engine. In Carnot cycle the working substance of the engine undergoes four successive changes: It receives heat (from the heat source) while expanding at high temperature, delivers work during a reversible adiabatic (no heat) expansion, rejects heat (to the heat sink) during a compression at low temperature, and finally receives work during a reversible adiabatic compression. The ratio of the net work output to the heat input, called the efficiency of a cyclical engine, is proportional to the difference between the temperatures of the heat source and the heat sink. Carnot asserted that it is the largest such ratio of any engine operating between the two temperatures. This assertion is known as Carnot's principle. It follows that an engine that produces work by exchanging heat with a single reservoir is impossible. Such an engine is called a perpetual motion machine of the second kind (PMM2). This definition is analogous to that of a perpetual motion machine of the first kind (PMM1) which produces work from nothing.

During the period from 1840 to 1848 James Prescott Joule showed experimentally that heat and work can produce the same effect on bodies when used in a fixed proportion. Thus, in a cyclic process, such as that of a cyclic engine, the net work produced must be proportional to the net heat received. He concluded that either heat or work results in a change of something stored in the bodies which is conserved. We now call that something energy.

In 1849 Lord Kelvin, a Scottish engineer, pointed out the conflict between the caloric basis of Carnot's argument in which heat (caloric) is conserved and the conclusion reached by Joule in which the sum of work and heat is conserved. Moreover, Joule's theory poses no limits on how much of the heat can be transformed into work, whereas Carnot's theory does. One year later, in 1850, Clausius reconciled Carnot's principle with the work of Joule by introducing the concept that bodies possess a property he called entropy having the following characteristics: In the absence of heat interactions with other bodies, it either remains constant if the body undergoes a reversible process, or increases. During heat interactions, on the other hand, the entropy of a body changes in proportion to the heat transferred to the body. It is this later characteristic that limits the efficiency of any work-producing cyclical engine, as required by Carnot's principle.

During the 50 years that followed Clausius, Maxwell, Planck and Poincaré completed the structure of thermodynamics and coined the terms Second Law for Carnot's principle and First Law for Joule's principle. The First Law asserts that the energy of an isolated body always remains the same. The Second Law, on the other hand, asserts that the entropy of an isolated body either stays fixed or increases but never decreases. Soon thereafter J. Willard Gibbs produced his famous paper on The Equilibrium of Heterogeneous Substances and brought the science of generalized thermodynamics to the same degree of perfection and comprehensive generality that Lagrange and Hamilton had in an earlier era brought to the science of generalized dynamics (The Scientific Papers of J. Willard Gibbs, 1906).

2. Statistical Mechanics

Concurrent with the development of thermodynamics as an axiomatic science was the development of the mechanical theory of heat which relates heat to changes in the motion of elementary particles of matter such as molecules. The history of that theory can be traced back to Democritus (c. 400 B.C.) and Epicurus (c.300 B.C.). The mechanical theory of heat, however, was not firmly established until Joule demonstrated experimentally that a quantitative relation exists between heat and work when they produce identical effects. In effect, Joule's finding directly relates the First Law of thermodynamics to Newton's laws of motion.

On the other hand, relating the Second Law to Newtonian mechanics proved more difficult. In particular a search to find what entropy meant within the framework of mechanics proved fruitless. As a result the scientific community at the time of Clausius believed that the Second Law applies only to macroscopic systems and, therefore, a way to find the meaning of entropy was by way of a new science called statistical mechanics. The essence of statistical mechanics is that most macroscopic bodies we study are too complicated for us to know their exact mechanical state at any given time and observations we make on these bodies represent averages either over time or space. The most we can know, therefore, at a particular time of the microscopic state of a physical body (system) is the probability of finding the system in that microscopic state.

The development of statistical mechanics can be traced through Helmholtz, Clausius, Maxwell, and Boltzmann. It culminated in the work of J. W. Gibbs who in 1901 presented an exposition of statistical mechanics that excels in completeness, rigor, and generality. Although Gibbs stated his exposition in terms of Newtonian mechanics, it is even better adapted to quantum mechanics, which in some ways it anticipates.

Perhaps because Gibbs' contribution was not fully understood, the less general and less rigorous approach of Maxwell and Boltzmann prevailed in the literature, with a few exceptions, until after World War II. A major contribution to the recent reawakening to Gibbs' methods is a book published by Erwin Schrödinger, in 1946, in which he explains the difference between the two approaches as follows: *"The older and more naïve application is to N actually existing physical systems in actual physical interaction with each other, e.g., gas molecules or electrons or Planck oscillators or degrees of freedom ... The N of them together represent the actual physical system under consideration. This original point of view is associated with the names of Maxwell, Boltzmann, and others.*

"But it suffices only for dealing with a very restricted class of physical systems – virtually only with gases. It is not applicable to a system which does not consist of a great number of identical constituents with 'private' energies. In a solid the interaction between neighboring atoms is so strong that you cannot mentally divide up its total energy into the private energies of its atoms. And even a 'hohlraum' (an 'ether block' considered as the seat of electromagnetic-field events) can only be resolved into oscillators of many – infinitely many – different types, so that it would be necessary at least to deal with an assembly of an infinite number of different assemblies, composed of different constituents.

"Hence a second point of view (or, rather, a different application of the same mathematical results), which we owe to Willard Gibbs, has been developed. It has a particular beauty of its own, is applicable quite generally to every physical system, and has some advantages to be mentioned forthwith. Here the N identical systems are mental copies of the one system under consideration – of the one macroscopic device that is actually erected on our laboratory table."

The essence of Gibbs' statistical mechanics can be summarized as follows: The state of a macroscopic system can be represented by an ensemble of N mental copies of the one system under consideration each at specified microscopic mechanical state s_i such that the percent frequency p_i of the members of the ensemble at a particular mechanical state is the probability that the macroscopic system is in that microscopic state. He then shows that the entropy S of the macroscopic system is

$$S = -k \sum_i (p_i \ln p_i) \quad \text{where} \quad \sum_i p_i = 1$$

In this way he relates the Clausius entropy to mechanics. In the limit, of course, when one of the p_i equals 1 all others are zero. It means there is 100% probability that the macro system is in a specific micro-state. Then the entropy of the system is zero.

The era of quantum mechanics began in 1901 with the publication by Max Planck of his work on the distribution law for black-body radiation. That same year Gibbs published his famous paper on statistical mechanics. It should be pointed out that although the mechanical states Gibbs refers to are Newtonian his analysis applies, without change, to quantum mechanical states as well.

3. Maxwell's Demon

Although statistical mechanics relates the thermodynamic entropy to mechanics two major conflicts between the two sciences remain. The first was pointed out by Maxwell in 1871 and is illustrated very clearly by what has come to known as Maxwell's demon.

Concerning this conflict, Maxwell comments as follows: *“One of the best established facts in thermodynamics is that it is impossible for a system enclosed in an envelope which permits neither change of volume nor passage of heat, and in which both the temperature and the pressure are everywhere the same, to produce any inequality of temperature or of pressure without the expenditure of work. This is the second saw of thermodynamics, and it is undoubtedly true so long as we can deal with bodies only in mass and have no power of perceiving or handling the separate molecules of which they are made up. But if we conceive a being whose faculties are so sharpened that he can follow every molecule in its course, such a being, whose attributes are still as essentially finite as a our own, would be able to do that which is at present impossible to us. For we have seen that the molecules in a vessel full of air at uniform temperature are moving with velocities by no means uniform though the mean velocity of any great number of them, arbitrarily selected, is almost exactly uniform. Now let us suppose that such a vessel is divided into two portions A and B, by a division in which there is a small hole, and that a being who can see the individual molecules opens and closed this hole, so as to allow only the swifter molecules to pass from A to B, and only the slower ones to pass from B to A. He will thus, without expenditure of work, raise the temperature of B and lower that of A, in contradiction to the Second Law of thermodynamics.”*

This conflict results from the fact that although mechanics allows under all circumstances the extraction of any fraction of the energy of any physical system confined within a given volume in the form of work, the Second Law limits the amount of work that can be extracted from such a system, depending on the value of a property called entropy, possessed by all systems in any specified condition. Only if the entropy of a system has the lowest value possible at the given energy, can all of its energy be extracted in the form of work. Under that condition, the laws of mechanics and thermodynamics become identical

The second conflict is stated by Gilbert N. Lewis in the following words: *“Willard Gibbs, in his early paper, first showed the incompatibility between molecular theory and the statement of classical thermodynamics that every system proceeds steadily toward a unique final state. We now have abundant experimental evidence that a system left to itself for an indefinite time assumes no single equilibrium state, but passed back and forth through a great number of different states which, however, are not easily distinguishable.”*

This second conflict arises from the fact that thermodynamics allows the possibility of irreversible processes such as those that make an isolated system in a non-equilibrium state spontaneously proceed to equilibrium in the long run. On the other hand, the equations of motion in both Newtonian and quantum mechanics are reversible.

The advent of the wave theory of matter (quantum mechanics) and, specifically, the introduction in 1927 of Heisenberg's principle of indeterminacy raised great hopes that the paradox posed by Maxwell's demon might be resolved and, moreover, that a complete proof of the Second Law of thermodynamics could be obtained based only on quantum-mechanical principles. Slater attempted the former and Watanabe the latter. Both attempts failed. Watanabe proved that it is impossible to deduce the Second Law from the principles of quantum mechanics without using a further postulate which in effect is equivalent to the Second Law.

4. Szilard's Resolution

Many scientists believe that the conflicts between thermodynamics and mechanics were resolved by Szilard in his famous paper of 1929, and Brillouin who in 1956 combined Szilard's concept with the information theory developed by Shannon in 1948.

Szilard's premise may be summarized as follows: We shall accept the proposition that it is possible to construct mechanical devices that make use of any one fluctuation of a system in stable equilibrium so as to produce work. Moreover, we shall accept the Second Law in the form that no net positive work may be obtained on the average from a system in stable equilibrium without producing any other effects on the environment. From these assumptions, we conclude that any instrument used to identify any given fluctuation of a system in stable equilibrium will absorb a quantity of work which is at least as much as the work that may be obtained from the fluctuation.

Szilard gives the following example. A molecule and is maintained cylindrical enclosure of volume V

contains one molecule and is maintained in equilibrium with a heat reservoir at temperature T . The cylinder is separated into two equal volumes by means of a sliding partition, and an instrument operating in a cycle and exchanging heat with the reservoir at T is used to identify which part contains the molecule. The partition is then operated as a piston and the part containing the molecule is expanded slowly against the evacuated part. From simple kinetics theory, we find that the average pressure, p , on the piston will be given by the perfect gas relation:

$$PV = C \quad \text{where } C \text{ is a constant.}$$

It follows that the work W done by the piston on the environment during the expansion from volume $V/2$ to volume V will be given by:

$$W = C \ln 2.$$

He concludes that by virtue of the Second Law the work received by the instrument in order to determine on which side of the partition the molecule is to be found must equal $C \ln 2$.

The information theory interpretation of the Second Law in effect implies that what we call the thermodynamic state of a physical body (system) is not an objective condition of the body but rather the information an observer possesses about the actual micro-state of the body. Such characterization not only attempts to resolve the first conflict mentioned (the impossibility of a PMM2) above but also the second. The evolution of a system from a non-equilibrium state towards equilibrium designates loss of information on the part of an observer.

5. My Involvement in Thermodynamics

While attending Athens Polytechnic the only subject I didn't like was Thermodynamics which, I was told consisted of two axioms, the First and Second Laws. The First Law, which in effect says that the change of energy of a system equals the heat received by it less the work done by it, appeared to me trivial. The Second Law, which in effect says that all of the heat extracted from a single body can not be transformed into work, appeared to me contrary to the laws of mechanics. Contributing to my dislike of thermodynamics was the fact that my aging professor was unable to answer my questions.

A year later, after arriving at MIT to study electronics, I decided to try again and take a course in thermodynamics to see if the thermodynamics professor there, Professor Joseph H. Keenan, made more sense than my professor in Greece. Professor Keenan was well known in engineering schools around the world for his clarity of thought and his emphasis on precise definitions of terms. His text book *Thermodynamics*, Wiley, New York, 1941 was adopted by most prominent engineering schools in both the United States and abroad. His other publications, *Mollier Diagram* (1930), *Thermodynamic Properties of Steam* (1938) and *Gas Tables* (1945), still occupy prominent places on the bookshelves of

engineers in the powerplant and chemical process industries.

After taking Professor Keenan's courses I was greatly impressed. Nevertheless, I only got hooked on to thermodynamics in 1950, after I pointed out my objections to his articulation of the Second Law.

In his classical book *Thermodynamics* (Keenan, 1941), professor Keenan adopted the statement of the Second Law proposed by M Planck in his *Treatise on Thermodynamics* (Planck, 1927), "*It is impossible to construct an engine which will work in a complete cycle, and produce no effect except the rising of a weight and cooling of a reservoir.*" *This statement constitutes the most widely used statement of the Second Law.*

I argued, as follows, that this statement is a tautology: The term reservoir in Planck's statement may mean a system in either stable equilibrium or not. If not, Planck's statement is incorrect, because one can always get work from a system in a non-equilibrium state or in a metastable state. If on the other hand it means a system in stable equilibrium, Planck's statement is true by the definition of a stable state. This is so because if one could cool the reservoir and get work, he could use that work to heat some part of the reservoir by friction, and thus have the reservoir change state while leaving no effect in the environment – a violation of what is meant by stable equilibrium.

After a long discussion, he agreed and then asked me to propose my own presentation. It took me ten years to complete Keenan's assignment. After many tries, I concluded that the Second Law is nothing different than a generalized statement that stable states exist. It may be expressed as follows: *A system having specified allowed states and an upper bound in volume can reach from any given state one and only one stable state and leave no net effects on its environment.*

I then showed that from this statement, one can derive not only all the corollaries of the Second Law but the First Law as well.

In 1959 Professor Keenan and I developed a new interpretation of thermodynamics that is applicable to a much wider range of systems and physical phenomena than any other interpretation presented in the past. This new interpretation applies to systems in nonequilibrium as well to equilibrium states, to systems having a few degrees of freedom, such as a single molecule, as well as systems with many degrees of freedom, such as a gas, quantum systems as well as classical systems, and systems undergoing nuclear as well as chemical reactions. It is presented in a book we coauthored, *Principles of General Thermodynamics*, published in 1965 (Hatsopoulos and Keenan, 1965) and adopted by the

graduate engineering schools of several major universities, both in the United States and abroad.

6. Physical Reality

About the time when the book “Principles of General Thermodynamics” was being completed, we began to have doubts about the information theory interpretation of thermodynamics and concluded that it is contrary to physical reality. In other words, it is wrong.

To illustrate the point consider the following situation: There is a room held at a constant temperature T_0 . We are told that in the room there are several identically constructed batteries, all at the same temperature--nothing else. Some of these batteries are charged and some are dead. The charged batteries can produce power, namely work, and the dead ones can not. From a thermodynamic point of view, the ones that are charged have lower entropy than the dead ones. I ask the question: can an observer having no further information determine which of these batteries are charged? Not only I believe the answer is a definitive yes, but also I believe we can experimentally determine how much charge its battery has and, therefore, calculate the difference in entropy between each of the charged batteries and the dead ones. Any logically thinking person, therefore, must conclude that entropy is an objectively determined property of these batteries.

Furthermore, other sciences such as physical chemistry and biology describe phenomena in terms of Gibbs chemical potential, a property which strongly depends on the partial entropy of a species in a mixture. Could we possibly imagine that the chemical potential of sodium ions in a living cell depends on the knowledge of an observer?

These concerns led us to the following conclusion: ***There are states of physical systems, such as stable equilibrium states, that are not describable by a single quantum mechanical wave function.***

7. A New Theory

In 1967, I teamed up with Elias Gyftopoulos, professor of nuclear engineering at MIT, to develop an axiomatic theory that includes all states of systems encountered in nature, and is entirely consistent with both quantum theory and the Second Law of thermodynamics.

The new theory is described in a four-part paper entitled “*A Unified Theory of Mechanics and Thermodynamics*” published in 1976 (Gyftopoulos and Gyftopoulos, 1976). It is derived from four postulates: Three are taken from quantum mechanics, and the forth is the following paraphrase of the

generalized statement of the Second Law: *Any independent and separable system subject to fixed parameters has for each set of (expectation) values of energy and of numbers of particles of constituent species a unique stable equilibrium state.*

Thus, the Second Law of Thermodynamics is presented as a fundamental proposition which is inviolable and not as one which arises from human inability or ignorance. Unlike information theory, it treats all probabilities related to the state of a system as objective characteristics of the system, and independent of the knowledge of an observer. In this theory the state of any system at any time is described by a Density Matrix (Density Operator) representing a Gibbs-type of ensemble of pure quantum states, each associated with a wave function, appearing in specific frequencies. These frequencies, in turn, represent probabilities that a state is describable by means of a single wave function associated with any one particular pure quantum state.

Newtonian mechanics stipulates that any physical body at any given time is in a particular mechanical state having specific positions and specific momenta for its constituent elementary particles. In contrast, quantum mechanics stipulates that the state of physical body at a given time can, at best, be described by a cloud of probabilities to find its particles in specific mechanical states. In other words, quantum theory postulates that the state of any physical system incorporates irreducible quantal dispersions that are inherent to it and can be described by means of a wave function.

The new theory goes one step beyond quantum mechanics. It stipulates that although a physical body can sometimes be found in conditions fully describable by means of wave function, as in pure quantum states, it can also be found, at other times, in conditions that incorporate broader quantal dispersions can at best be described by a cloud of probabilities to find it in any one particular quantum state. The uncertainties associated with such states, therefore, are much larger than those associated with pure quantum states. An example of these latter conditions is the state of stable equilibrium.

8. Reactions of the Scientific Community to the New Theory

With few exceptions, the reaction of the scientific community to the new theory was mostly non-committal and occasionally negative. The exceptions include Professor Henry Margenau (The Eugene-Higgins Professor of Physics and Natural Philosophy at Yale University) of Yale University, Professor J. H. Keenan of MIT, and Professor James Park of Washington State University. Their views are described below:

• In a letter of March 19, 1974 to Professor Louis De Broglie of the French Academy of Sciences, Professor Henry Margenau wrote: *“The [Hatsopoulos-Gyftopoulos] paper presents the Second Law of thermodynamics as a fundamental axiom deeply embedded in quantum theory and connects the two disciplines in a way previously unknown to me. And it sheds new light on the Second Law presenting it as a proposition which is inviolable, not as one which arises from human inability or ignorance.*

“It treats the probabilities of quantum mechanics as objective, independent of the knowledge of an observer. In view of the current trend, induced by the successes of information theory, which reduced thermodynamics to matters of what an observer knows, the seemingly flawless arguments of this article are to me encouraging. “It rejects von Neumann’s projection postulate; indeed it shows that if this axiom is used the attempted unification does not occur. At this point I speak with a personal bias, for I have tried to expose this postulate as invalid and useless for some 40 years. An early discussion with Einstein convinced me and him that I was on the right track. But while the literature does show diminishing reliance on this strange phenomenon of “collapse of a wave packet”, most textbooks still feature it as a necessary ingredient of wave mechanics. It makes sense only in connection with a subjective interpretation of quantum mechanics, an interpretation which reduces physics to psychology.

“The paper leads to the astonishing but fascinating conclusion that the customary quantum mechanical equation of motion is not universal, suggesting that the prevalent formulation of quantum mechanics may not be complete or indeed correct...”

• In a letter of March 12, 1974 to Professor Eugene P. Wigner of Princeton University, Professor Joseph H. Keenan wrote:

“Entropy in classical thermodynamics is related to “the available work of the body and medium” (Gibbs, Collected Works, Vol. 1, p. 53) as well as to the impossibility of a perpetual motion machine of the second kind. No such concept as available work arises from mechanics.

“When Hatsopoulos and I wrote our ‘Principles of General Thermodynamics’ in 1965 we attempted to resolve the difficulty by means of Szilard’s ideas about information and negentropy. We have since become convinced that this explanation is defective in that it does not show how work can be obtained from a system that is far from equilibrium with the environment, such as fossil fuel, by a person who approaches the system with no previous information about it. The theory of Hatsopoulos and Gyftopoulos claims that this work is determined by irreducible quantal dispersions of results of

measurement that are inherent in the nature of a system.

“Instead of being a measure of our ignorance, in this theory a nonzero value of entropy becomes a measure of irreducible quantal dispersions of results of measurement associated with mixed states. The mixed states in question are operationally defined, objective, and irreducible to mixtures of other states.

“Any subjective imperfection of knowledge about the state results in the need to consider additional dispersions which must be superimposed on those that are inherent to quantum physics. It is this subjective ignorance with which the anthropomorphic interpretation of thermodynamics is principally concerned but which is related to the basic unavailability of energy which is the essence of the Second Law. The unavailability is related only to irreducible quantal dispersions associated with results of measurements and in no sense involves the knowledge of an individual observer. Beyond the irreducible dispersions considered by von Neumann in connection with pure states, the authors prove the existence of irreducible dispersions associated with mixed states and these dispersions express the basic implications of the Second Law of classical thermodynamics.”

- In a letter of June 18, 1974 to The Physical Review Professor James Park wrote: *“Beyond question this [HatsopoulosGyftopoulos] paper contains profound new content. The unified theory constructed in the paper contradicts nothing in experience. Yet it does point the way toward the resolution of contradictions which at present do exist (despite extravagant claims of information theorists) between orthodox quantum mechanics and thermodynamics. Especially noteworthy is an original analysis of state preparation which establishes the necessity and probes the heretoforth uninvestigated possibility that a mixed density operator may describe an ensemble physically irreducible to pure constituents. That such a quantal discovery should occur in the context of thermodynamical argument is fascinating, for it is somewhat reminiscent of the role of thermodynamics in the early history of quantum mechanics.”*

9. Concluding Remarks

The discussion given above leads to the following conclusions: (1) The Second Law is probably as universally valid as is the First Law, namely the conservation of energy, and (2) Entropy is not a subjective property of a system related to what an observer knows about it but an objective and measurable property of any system in any state.

The Second Law restrictions have enormous practical importance. The human needs for energy relate

almost exclusively to work: Work is needed to power our vehicles, to produce electricity, to cool an environment to below ambient temperature, to heat an environment to above ambient temperature, and to perform a multitude of physical or chemical transformations in the processing of materials. The only human needs that don't require work are to heat or cool something to ambient temperature. Every other need requires work. The ultimate solution to the energy need of our society, therefore, is to invent a machine that draws upon the enormous energy existing in our environment and produces work. Such a machine is called the perpetual motion machine of the second kind (PMM2), which, unlike the perpetual motion machine of the first kind (PMM1), does not violate the law of conservation of energy.

Still, a literature review reveals that most physicists from 1850 to the mid 20th century believed that the prohibition of Second Law is not absolute, but merely reflects limitations of the prevailing state of micro-technology. After that period most physicists still believe the prohibition does not relate to the objective condition of a system but rather reflects lack of knowledge of the observer.

In contrast to physicists, virtually all engineers reject both these explanations and believe that the impossibility of a PMM2 is an irrefutable law of nature. In other words they believe that entropy is an objective property of any physical system that can never decline unless the entropy of another system increases by at least the same amount. This view prevailed to such an extent that, although enormous effort is constantly made to find new sources of energy, no organized activity to develop a PMM2 has ever been undertaken. In fact the US Patent Office has ruled that any invention violating the Second Law be rejected. In this connection, one may mention, somewhat facetiously, that a US Congressman once objected to this ruling on the grounds that the U.S. Congress had never, to his knowledge, passed any law called The Second Law of Thermodynamics.

9.1 An unanswered question

The Hatsopoulos-Gyftopoulos theory resolves the conflict pointed out by Maxwell but not the one pointed out by Gilbert N. Lewis. The latter results from the fact that thermodynamics permits, but does not mandate, irreversible processes that increase the sum of the entropies of all systems involved. Yet the equation of motion, we know, is reversible. Margenau comments in his letter to DeBroglie: *"The paper [by Hatsopoulos-Gyftopoulos] leads to the astonishing but fascinating conclusion that the customary quantum mechanical equation of motion is not universal,..."*

The question arises whether we need to devise a more general equation of motion that permits irreversible processes. It is very difficult to answer this question because we don't know what makes a process irreversible. All we actually know for a fact is that in the absence of heat and work interactions,

a condition we call isolation, a system sometimes proceeds towards equilibrium at constant energy and, therefore, its entropy increases. On that basis we conclude that irreversible processes exist.

9.2 Developments after 1976

In 1979 a doctoral student of Elias Gyftopoulos, Gian Paolo Beretta, joined our team and after two years came up with an equation of motion that satisfies the long list of necessary properties for it to be compatible with the unified theory, including the feature that it reduces exactly to the Schrödinger equation for states that can be described by a single wave function. The Beretta equation implies a spontaneous and irreversible tendency of the cloud of probabilities that describe the state of an isolated system to rearrange themselves so as to increase the entropy at constant energy until eventually an equilibrium distribution is reached, which turns out to be dynamically stable. Thus, by postulating this equation of motion in the unified theory, our generalized statement of the second law becomes a theorem. Gyftopoulos, Beretta and coworkers have proved (Beretta et al., 1984) several other mathematical and physical features, including proofs of Onsager reciprocity and steepest-entropy-ascent theorems. The theory, now completed with a dynamical principle that entails the second law, prompted the encouraging reactions outlined above.

Since then, with few exceptions, the theory has been almost ignored, until in 2001 it was literally ‘rediscovered’ by Gheorghiu-Svirschevski who published a paper in the *Physical Review A* (Gheorghiu-Svirschevski, 2001a) entitled “*Nonlinear quantum evolution with maximal entropy production*” in which he proposes “that a physically meaningful nonlinear extension emerges when the fundamental postulates of quantum mechanics are supplemented by the first and second principles of thermodynamics, at the sole expense of ignoring the constraint of a linear, unitary evolution in time” and derives the Beretta equation from a maximal entropy production variational principle entirely equivalent to the original steepest entropy ascent hypothesis. Although this paper makes no reference to any of our original papers, an Addendum published soon after in *Physical Review A* by the same author (Gheorghiu-Svirschevski, 2001b) acknowledges his oversight of our pioneering contributions. What is important is that recent advances in technology and laboratory techniques towards micro-devices and experimental setups have moved the interest of the physical community towards the microscopic world, where the implications of thermodynamics still hold. Therefore, slowly, there appears to have been a drift towards reformulations of the statistical mechanics and the information theory approaches that tend to gradually incorporate the fundamental hypothesis presented in this paper.

References

-
-
- The Scientific Papers of J. Willard Gibbs, Longmans, Green, and Co., 1906.*
- Beretta, G. P., Gyftopoulos, E. P., Park, J. L., and Hatsopoulos, G. N., 1984, Nuovo Cimento B, Vol. 82, 169; G.P. Beretta, G. P., Foundations of Physics, Vol. 17, 365 (1987) and references therein.*
- Gheorghiu-Svirschevski, S., 2001a, Physical Review A, Vol. 63, 022105.*
- Gheorghiu-Svirschevski, S., 2001b, Physical Review A, Vol. 63, 054102.*
- Hatsopoulos, G. N. and Keenan, J. H., 1965, Principles of General Thermodynamics, John Wiley & Sons, Inc., New York - London - Sydney.*
- Hatsopoulos, G. N. and Gyftopoulos, E. P., 1976, "A Unified Theory of Mechanics and Thermodynamics," Foundations of Physics, Vol. 6, 15, 127, 439, 561.*
- Keenan, J. H., 1941, Thermodynamics, John Wiley & Sons, Inc., New York-London-Sydney. Planck, M., 1927, Thermodynamics, Longmans, Green, London.*

Thermodynamic Optimization of GSHPS Heat Exchangers*

Javad Marzbanrad**, Ali Sharifzadegan and Ahmad Kahrobaeian
Automotive Engineering Department
Iran University of Science and Technology, Tehran - Iran
Email: marzban@iust.ac.ir

ABSTRACT

In this paper, a new method for determining the optimized dimensions of a ground source heat pump system (GSHPS) heat exchanger is presented. Using the GSHPS is one of the ways for utilization of infinite, clean and renewable energies in the environment. In recent years, due to limitation of physical space for installing the heat exchangers and avoiding the environmental effects on heat exchanger operation, vertical GSHP systems are used more than the other ones. Determination of optimum heat exchanger size is one of the most important parameters in the optimization of the heat exchanger design. In this study, optimum length and diameter for the heat exchanger is determined for different mass flows by using the second law of thermodynamics. The optimal length and diameter minimize entropy generation and therefore result in increased efficiency of the heat pump.

Keywords: GSHP, ground source heat pump, heat exchanger, entropy minimization, thermodynamical design.

1. Introduction

The natural environments contain unlimited resources of energy at low exergy levels. This energy is very cheap or even free. Hence the interest in its utilization increases with the increasing costs or inconvenience of obtaining the highly exergetic energy. The utilization of these resources is possible by using heat pumps. The principles of operation of heat pumps are similar to refrigeration equipment. One of the most interesting research fields in the study of heat exchangers is to find methods to increase the heat pump's efficiency. Most heat pumps are used for the heating or cooling of residential buildings. In these cases, air and soil are usually the only available resources and utilization of underground or surface water is usually impossible. There are three loops in each GSHP:

- a) The first loop, with regard to its application, is an air/water or air/air loop which transfers heat from the warmer to the colder area.
- b) The second loop is the refrigerant cycle.

c) The third loop is the ground heat exchanger which transfers heat from the ground/heat exchanger to the heat exchanger/ground.

The GSHPs is used more often than air types, because the ground source or sink temperature is more stable than the air temperature over time (Claesson and Eskilson, 1987).

In the GSHP, heat absorption is done by circulating the working fluid in the heat exchanger. This working fluid can be pure water, a mixture of water and anti-freeze, or brine that usually circulates in the high density polyethylene (HDPE) pipes installed vertically in boreholes (VGSHP) or horizontally in grooves (HGSHP).

HGSHPs are not commonly used in houses because these systems need more space for installation than the VGSHP and temperature variations have greater effects on them. As shown in Figure 1, in VGSHP systems, the heat exchanger usually consists of two or more boreholes (with depths between 20 and 90 meters). There is a u-tube in each borehole and the boreholes are filled with grout.

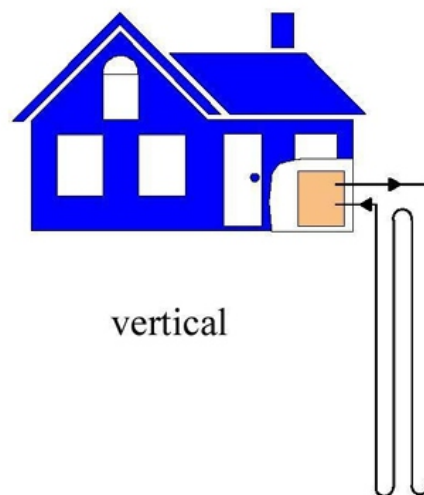


Figure 1. A vertical ground source heat pump

In recent years, many analytic and numeric methods for the determination of u-tube sizes have been presented (Chiasson, 1999). The purpose of a thermodynamic design is to achieve a working system. A goal of the design is high efficiency; minimization of entropy production is a way to achieve this. For the determination of the u-tube optimum sizes, the total generated entropy should be minimized in the heat exchanger because, for a given heating load, there is a direct relationship between entropy generated and the required power input.

In this paper, the temperature distribution along the u-tube is analytically determined, and then with regard to the second law of thermodynamics, an equation is presented for the calculation of the generated entropy in the heat exchanger. By using this equation, the optimum Reynolds number and therefore the optimum length and diameter of the heat exchanger is determined. Finally an example application of this method is presented along with results and related figures.

2. Entropy generation through internal flows

The irreversibility of convective heat transfer is due to two effects (Bejan, 1988): a) heat transfer across a finite (non-zero) temperature difference, b) fluid friction.

Considering the flow passage through arbitrary cross section A and the wetted perimeter P, bulk properties of the stream m are T, h, s and p when heat is transferred to the stream at a rate q' [W/m], across a finite temperature difference. Focusing on a slice of thickness dx as a system, the rate of entropy generation is found with an entropy balance:

$$d\dot{S}_{gen} = \dot{m}ds - \frac{qdx}{T + \Delta T} \quad (1)$$

\dot{S}_{gen} on the Stanton number and friction factor information, consider the case where the heat transfer rate per unit length q' and the mass flow rate m are specified; combining definition with formula yields:

$$\dot{S}'_{gen} = \frac{q'^2}{4T^2 \dot{m} C_p} \cdot \frac{D}{St} + \frac{2\dot{m}^3}{\rho^2 T} \cdot \frac{f}{DA^2} \quad (2)$$

where

$$St = \frac{h}{\rho V C_p}$$

Under the present assumptions, Eq. (2) has two degrees of freedom, the wetted perimeter P and the cross-sectional area A or any other couple of independent parameters such as (ReD, D). In a round tube of diameter D, the rate of entropy generation per unit length Eq. (2), assumes the form:

$$\dot{S}'_{gen} = \frac{q'^2}{\pi k T^2 Nu ((Re)_D, Pr)} + \frac{32 \dot{m}^3}{\pi^2 \rho^2 T} \cdot \frac{f((Re)_D)}{D^5} \quad (3)$$

Note that Eq. (3) depends on only one geometric parameter [D or (Re)D]. As the tube diameter increases, (Re)D decreases; the interesting effect on \dot{S}'_{gen} is that while the heat transfer contribution increases, the fluid friction term decreases. This is one example in which a variation of one geometric

parameter always has opposite effects on the two terms of S_{gen} . Consequently, it is possible to determine the optimum tube diameter, or $(Re)_D$, which leads to minimum irreversibility. If the pipe flow is turbulent and fully developed, the Nusselt number and friction factor are given by the well known correlations:

$$Nu = 0.023[(Re)_D]^{0.8} (Pr)^{0.4}$$

$$f = 0.046 [(Re)_D]^{-0.2}$$

Combining this formula with Eq. (3) yields (Bejan, 1994):

$$\dot{S}_{gen} = \left(\frac{43.48 q^2}{\pi k T^2 Pr^{0.4}} \right) Re^{-0.8} + \left(1.44 \times 10^{-3} \right) \left(\frac{\pi^3 \mu^5}{\rho^2 T \dot{m}^2} \right) Re^{4.8} \quad (4)$$

3. Determination of entropy generated in the Utube

For determination of entropy generated in the u-tube heat exchanger, we shall first determine the temperature distribution along the u-tube. Considering Eq. (4), as is illustrated in Figure 2 and shown in Eq. (5), the heat exchanger consists of two heat fluxes which are absorbed by working fluid in the heat exchanger: dq_{con} due to heat transfer from ground and dq_{int} due to heat transfer between the warmer and colder branches of utube.

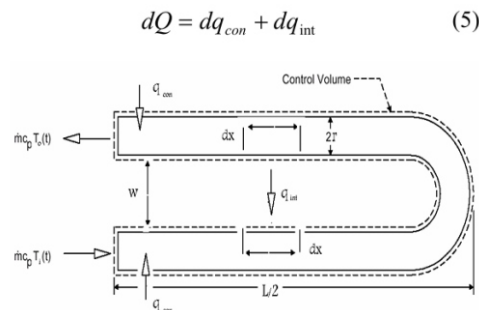


Figure 2. Heat fluxes in the u-tube heat exchanger

4. Heat flux due to heat transfer from ground

The ground temperature changes at the zones around the heat exchanger (Rybach, and Sanner, 2000):

First, when the heat pump starts its operation, the ground temperature decreases and after time, the ground temperature reaches a new stable temperature which is 1 to 2 Kelvin lower than the original temperature.

Second, the ground temperature changes decrease, as the distance from the heat exchanger increases. At

distances greater than 5 to 10 meters from the heat exchanger, the temperature changes are less than 1 Kelvin.

To determine the heat flux due to heat transfer from the ground, we can assume the heat flux is absorbed by the heat exchanger radially at steady state heat conduction. We can divide the area around the heat exchanger into three coaxial cylinders whose radii are r_1 (u-tube radius), r_2 (borehole radius) and r_3 (the position where the ground temperature is not affected by the heat exchanger).

The heat transfer coefficient can be found with Eq. (6). With a known heat transfer coefficient, the heat flux can be found with $q_{con} = h_t(T_{\infty} - T)$ (Holman, 1997).

$$h_t = \frac{1}{\sum_{i=1}^3 \frac{r_1}{k_i} \ln \frac{r_i}{r_{i-1}}} \quad (6)$$

5. Heat Transfer between Two Branches of a U-tube

In a u-tube heat exchanger, heat transfer occurs due to temperature differences between the two branches of the u-tube. The u-tube heat exchanger can be modeled as two very long cylinders (which are parallel at a distance equal to W) in an infinite media (ground). With reference to Figure 2, the heat flux can be determined.

$$q_{int} = SK[T(x) - T(L - x)] \quad (7)$$

where:

$$S = \frac{2\pi L}{\cosh^{-1}\left(\frac{2W^2}{r^2}\right)} \quad (8)$$

6. Temperature Distribution along U-Tube

By writing the energy equation in a differential element of the u-tube of length dx (Figure 3), we have:

$$dQ = -m dh \quad (9)$$

where:

$$dh = c_p dT$$

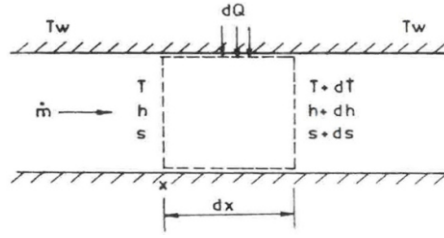


Figure 3. Differential element of the u-tube

The absorbed heat flux (dQ) consists of two fluxes, (dq_{con} due to heat absorbed from ground and dq_{int} due to heat transferred between the two branches of the u-tube), so by using the previously mentioned material, we can determine dq_{con} :

$$dq_{con} = h_i 2\pi r dx \theta \quad (10)$$

By substitution, Eqs. (7), (8) and (10) into Eq. (5) and solving the resulting nonhomogeneous differential equation, the temperature distribution along the u-tube is found (Mukherjee, 1987):

$$\theta = (\theta_i - b) \exp(-az) + b \quad (11)$$

where:

$$z = xr$$

$$a = \frac{h_i 2\pi}{\dot{m} c_p}$$

$$b = \frac{-KQ}{2 h_i \dot{m} c_p \cosh^{-1} \left(\frac{2W^2}{r^2} \right)}$$

7. Entropy Minimization in the Heat Exchanger

By using the temperature distribution given by Eq. (11) and substituting it into Eq (4), the generated entropy in the heat exchanger can be written in terms of the Reynolds number. By differentiating this with respect to the Reynolds number and equating it to zero, the optimum Reynolds number can be determined:

$$Re_{opt} = (2.626) \left(\frac{M}{N} \right)^{0.131} (Pr)^{-0.053} B_o^{0.263} \quad (12)$$

where:

$$B_o = \frac{h_i \dot{m}^{\frac{3}{2}} \rho}{k^{\frac{1}{2}} \mu^{\frac{7}{2}}}$$

$$N = \int_0^n \frac{dz}{T}$$

$$M = \int_0^n \frac{\Delta T}{T^2} dz$$

$$dz = r dx$$

$$n = rL$$

By using Reopt, optimum length and diameter for the u-tube can be determined.

8. The generated entropy due to the heat transfer between the two branches of the Utube

Heat transfer between the two branches of the u-tube increases the entropy in the heat exchanger (as shown in Fig. 2). Generated entropy in a slice of thickness dx can be written:

$$\dot{S}'_{\text{int}} = \frac{q_{\text{int}}}{T(x)} - \frac{q_{\text{int}}}{T(L-x)} = q_{\text{int}} \left[\frac{1}{T(x)} - \frac{1}{T(L-x)} \right] \quad (13)$$

where:

S' int is the generated entropy due to heat transfer between the two u-tube branches.

By adding this equation to the above mentioned equations and differentiating with respect to the Reynolds number, Eq. (12) can be modified to Eq. (14) with an additional term A3 as follows, when considering the heat transfer between the two u-tube branches:

$$A_1 \text{Re}_{\text{opt}}^{-2.8} - A_2 \text{Re}_{\text{opt}}^{4.8} + A_3 = 0 \quad (14)$$

where:

$$A_1 = \frac{626.112 M h_i^2 \dot{m}}{\mu k \text{Pr}^{0.4}}$$

$$A_2 = \left(4.176 \times 10^{-3} \right) \left(\frac{\pi^4 \mu^6 N}{\rho^2 \dot{m}^2} \right)$$

$$A_3 = \frac{\pi^2 \mu k Q^2 n}{4 \dot{m}^3 C_P^2} \left(\frac{1}{T_1 T_2} \right) \left(\frac{1}{\cosh^{-1} \left(\frac{2W^2}{r^2} \right)} \right)$$

Note that if heat transfer between the two branches of the u-tube is not considered and the A_3 term deleted, Eq. (14) will change to the simpler form of Eq. (12).

9. Results

As an example, consider a u-tube with a oneinch diameter as a heat exchanger installed in a borehole, and assume the surrounding area is filled with grout and sand. If we divide the area around the u-tube into three zones, where the geometric and thermophysical characteristics of these zones are as described in Table I:

TABLE I. GEOMETRIC AND THERMOPHYSIC CHARACTERS OF THE ZONES AROUND THE U-TUBE HEAT EXCHANGER

material	heat conductivity [W/m K]	zone radius [m]
u-tube pipe (HDPE)	0.33	0.0301
grout	1.8	0.1
soil	2.5	5

The distance between two branches of u-tube is $W=0.114$ m. With the information presented in Table 1, the total heat transfer coefficient can be obtained:

$$h_t = 14.43 \text{ } W / m^2 K \quad (15)$$

The ground and fluid entrance temperatures are $T_\infty = 293$ K and $T_i = 283$ K, respectively. With water as a working fluid in the u-tube, and assuming the water physical properties do not change with temperature, the thermophysical properties are as follows:

$$C_p = 4200 \text{ } J / kgK$$

$$\rho = 999.8 \text{ } kg / m^3$$

$$\mu = 70 \times 10^{-5} \text{ } pas$$

$$Pr = 10$$

Considering the u-tube as a control volume and applying the first law of thermodynamics as well as Equation (11), n can be determined:

$$n = \left(\frac{-1}{a} \right) \ln \left[\frac{Q}{\dot{m} c_p (\theta_i - b)} + 1 \right] \quad (16)$$

By using n and Equation (12), the optimum Reynolds number and then the optimum u-tube length and diameter can be found for different mass flow and heat loads. In order to do this, two integrals, M and N , are calculated numerically. The results are presented as graphs in Figures 4 and 5. Eq. (14) is a nonlinear equation, therefore Re_{opt} is found through numeric methods. The optimum u-tube length and diameter for different mass flows and heat loads are shown in Figures 4 and 5 with dashed lines.

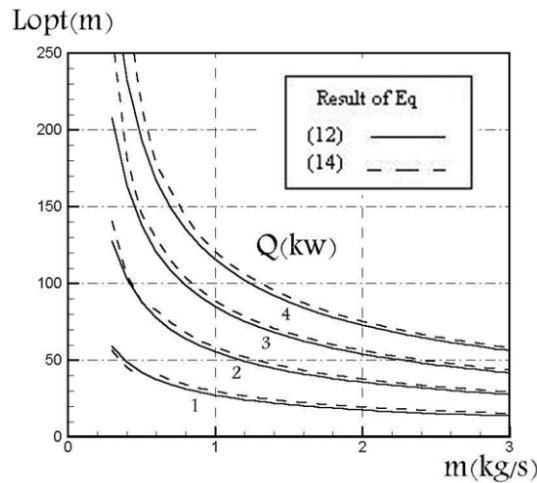


Figure 4. Optimum length vs. mass flows for different heating loads

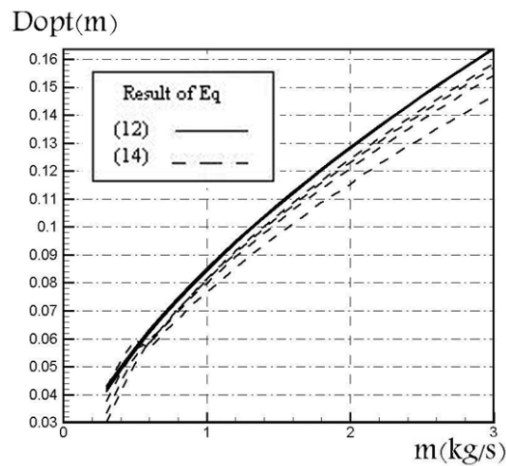


Figure 5. Optimum diameter vs. mass flows for different heating loads

10. Conclusion

By using the method presented in this paper, and therefore minimizing the entropy generated in the heat exchanger, optimum u-tube length and diameter can be determined. Thus less exergy is destroyed, less

power is required for a given duty, and the heat pump efficiency increases. In this method, heat exchanger optimum sizes can be determined; if we have circulation pump characteristics, then the proper mass flow is selected for it using the graphs presented.

Figure 4 shows that the optimum u-tube length decreases when the mass flow increases or when the heating load increases. Figure 5 shows that the optimum u-tube diameter increases when the mass flow increases. However, increased heating loads have no significant effect. The dashed lines in Figures 4 and 5 compare the difference between the solutions using Eq. (14) (considering the effects of u-tube branches on each other) and those using Eq. (12). Considering the dashed lines in Figures 4 and 5, it can be seen the solution of the non-linear Eq. (14) can be avoided. The difference between the two solutions is negligible. In recent years, many different analytic and numeric methods have been presented for designing a heat pump's u-tube heat exchanger, and there is much software based on them. The method presented in this paper is for the optimization of the heat exchanger sizes with regard to the second law of thermodynamics. This method can also be used with available software and incorporates the second law of thermodynamics into the design of GSHP heat exchangers.

Nomenclature

A	surface area [m^2]
a	constant parameter
b	constant parameter
B_0	duty parameter
C_p	heat capacity [J/kgK]
D	hydraulic diameter
f	friction factor
h	enthalpy of working fluid [kJ/kg]
h_t	total heat transfer coefficient [$\text{W/m}^2\text{K}$]
K, k_i	thermal conductivity [W/mK]
L	length of u-tube [m]
M	duty parameter
\dot{m}	mass flow rate [kg/s]
N	duty parameter
n	duty parameter
Nu	Nusselt number
Pr	Prandtl number
Q	total heat transfer rate [W/m]
q	local heat transfer rate [W/m]
r	radius of u-tube [m]
Re	Reynolds number
S	shape factor
S_{gen}	rate of entropy generation [W/mK]
St	Stanton number
T	temperature [K]
W	distance between u-tube branches [m]
z	$-r \times$
ρ	density [kg/m^3]
μ	viscosity [kg/sm]
θ	$T - T_{\infty}$

References

- Bejan, A., 1988, Advanced Engineering Thermodynamics, John Wiley & Sons, New York.*
- Bejan, A., 1994, Entropy Generation through Heat and Fluid Flow, John Wiley & Sons, New York.*
- Chiasson, A. D., 1999, "Advances in Modeling of Ground Source Heat Pump Systems", Master of Science Theses, Graduate College of Oklahoma State University.*
- Claesson, J. and Eskilson, P., 1987, "Thermal Analysis of Heat Extraction Bore Holes", 264 p., PhD-thesis, Lund-MPh-87/13, Lund University of Technology, Sweden.*
- Eugster, W. J. and Rybach, L., 2001, "Long Term Performance and Sustainability of Borehole Heat Exchanger Systems - the Swiss Experience", Zeitschrift Geothermische Energie, Geothermische Energie 32/33, March/June.*
- Holman, J. P., 1997, Heat Transfer, Eight Edition, McGraw Hill, Inc.*
- Lund, J. W., 2002, "Design of Closed Loop Geothermal Heat Exchangers in the U. S.", International Course on Geothermal Heat Pumps, Chapter 2.4, pp. 135-146.*
- Mukherjee, P., 1987, "Thermodynamic Optimization of Convective Heat Transfer through a Duct with Constant Wall Temperature", Int. J. Heat and Mass Transfer, Vol. 30, No. 2, pp. 401-405.*
- Phetteplace, G., Kavanaugh, S., 1998, "Design of Issues for Commercial Scale Ground Source Heat Pump Systems", Heartland Technology Transfer Conference, June 1-4, Kansas City, MO. Washington, DC.*
- Rybach, L. and Sanner, B., 2000, "Ground Source Heat Pump Systems' the European Experience", GHC (GEO-HEAT CENTER), Oregon Institute of Technology, Bulletin, pp. 16-26.*

Instructions for Authors

Essentials for Publishing in this Journal

- 1 Submitted articles should not have been previously published or be currently under consideration for publication elsewhere.
- 2 Conference papers may only be submitted if the paper has been completely re-written (taken to mean more than 50%) and the author has cleared any necessary permission with the copyright owner if it has been previously copyrighted.
- 3 All our articles are refereed through a double-blind process.
- 4 All authors must declare they have read and agreed to the content of the submitted article and must sign a declaration correspond to the originality of the article.

Submission Process

All articles for this journal must be submitted using our online submissions system. <http://enrichedpub.com/> . Please use the Submit Your Article link in the Author Service area.

Manuscript Guidelines

The instructions to authors about the article preparation for publication in the Manuscripts are submitted online, through the e-Ur (Electronic editing) system, developed by **Enriched Publications Pvt. Ltd.** The article should contain the abstract with keywords, introduction, body, conclusion, references and the summary in English language (without heading and subheading enumeration). The article length should not exceed 16 pages of A4 paper format.

Title

The title should be informative. It is in both Journal's and author's best interest to use terms suitable. For indexing and word search. If there are no such terms in the title, the author is strongly advised to add a subtitle. The title should be given in English as well. The titles precede the abstract and the summary in an appropriate language.

Letterhead Title

The letterhead title is given at a top of each page for easier identification of article copies in an Electronic form in particular. It contains the author's surname and first name initial .article title, journal title and collation (year, volume, and issue, first and last page). The journal and article titles can be given in a shortened form.

Author's Name

Full name(s) of author(s) should be used. It is advisable to give the middle initial. Names are given in their original form.

Contact Details

The postal address or the e-mail address of the author (usually of the first one if there are more Authors) is given in the footnote at the bottom of the first page.

Type of Articles

Classification of articles is a duty of the editorial staff and is of special importance. Referees and the members of the editorial staff, or section editors, can propose a category, but the editor-in-chief has the sole responsibility for their classification. Journal articles are classified as follows:

Scientific articles:

1. Original scientific paper (giving the previously unpublished results of the author's own research based on management methods).
2. Survey paper (giving an original, detailed and critical view of a research problem or an area to which the author has made a contribution visible through his self-citation);
3. Short or preliminary communication (original management paper of full format but of a smaller extent or of a preliminary character);
4. Scientific critique or forum (discussion on a particular scientific topic, based exclusively on management argumentation) and commentaries. Exceptionally, in particular areas, a scientific paper in the Journal can be in a form of a monograph or a critical edition of scientific data (historical, archival, lexicographic, bibliographic, data survey, etc.) which were unknown or hardly accessible for scientific research.

Professional articles:

1. Professional paper (contribution offering experience useful for improvement of professional practice but not necessarily based on scientific methods);
2. Informative contribution (editorial, commentary, etc.);
3. Review (of a book, software, case study, scientific event, etc.)

Language

The article should be in English. The grammar and style of the article should be of good quality. The systematized text should be without abbreviations (except standard ones). All measurements must be in SI units. The sequence of formulae is denoted in Arabic numerals in parentheses on the right-hand side.

Abstract and Summary

An abstract is a concise informative presentation of the article content for fast and accurate Evaluation of its relevance. It is both in the Editorial Office's and the author's best interest for an abstract to contain terms often used for indexing and article search. The abstract describes the purpose of the study and the methods, outlines the findings and state the conclusions. A 100- to 250-Word abstract should be placed between the title and the keywords with the body text to follow. Besides an abstract are advised to have a summary in English, at the end of the article, after the Reference list. The summary should be structured and long up to 1/10 of the article length (it is more extensive than the abstract).

Keywords

Keywords are terms or phrases showing adequately the article content for indexing and search purposes. They should be allocated heaving in mind widely accepted international sources (index, dictionary or thesaurus), such as the Web of Science keyword list for science in general. The higher their usage frequency is the better. Up to 10 keywords immediately follow the abstract and the summary, in respective languages.

Acknowledgements

The name and the number of the project or programmed within which the article was realized is given in a separate note at the bottom of the first page together with the name of the institution which financially supported the project or programmed.

Tables and Illustrations

All the captions should be in the original language as well as in English, together with the texts in illustrations if possible. Tables are typed in the same style as the text and are denoted by numerals at the top. Photographs and drawings, placed appropriately in the text, should be clear, precise and suitable for reproduction. Drawings should be created in Word or Corel.

Citation in the Text

Citation in the text must be uniform. When citing references in the text, use the reference number set in square brackets from the Reference list at the end of the article.

Footnotes

Footnotes are given at the bottom of the page with the text they refer to. They can contain less relevant details, additional explanations or used sources (e.g. scientific material, manuals). They cannot replace the cited literature.

The article should be accompanied with a cover letter with the information about the author(s): surname, middle initial, first name, and citizen personal number, rank, title, e-mail address, and affiliation address, home address including municipality, phone number in the office and at home (or a mobile phone number). The cover letter should state the type of the article and tell which illustrations are original and which are not.